HHS Public Access

Author manuscript

J Comp Neurol. Author manuscript; available in PMC 2016 June 15.

Published in final edited form as:

J Comp Neurol. 2015 June 15; 523(9): 1359–1378. doi:10.1002/cne.23740.

In vivo clonal overexpression of neuroligin 3 and neuroligin 2 in neurons of the rat cerebral cortex. Differential effects on GABAergic synapses and neuronal migration

Christopher D. Fekete, **Tzu-Ting Chiou**, **Celia P. Miralles**, **Rachel S. Harris**, **Christopher G. Fiondella**, **Joseph J. LoTurco**, and **Angel L. De Blas**

Department of Physiology and Neurobiology, University of Connecticut, Storrs, Connecticut, 06269, USA

Abstract

We have studied the effect of clonal overexpression of neuroligin 3 (NL3) or neuroligin 2 (NL2) in the adult rat cerebral cortex following *in utero* electroporation (IUEP) at embryonic stage E14. Overexpression of NL3 leads to a large increase in vGAT and GAD65 in the GABAergic contacts that the overexpressing neurons receive. Overexpression of NL2 produced a similar effect but to a lesser extent. In contrast, overexpression of NL3 or NL2 after IUEP, does not affect vGlut1 in the glutamatergic contacts that the NL3 or NL2 overexpressing neurons receive. The NL3 or NL2 overexpressing neurons do not show increased innervation by parvalbumin-containing GABAergic terminals or increased parvalbumin in the same terminals that show increased vGAT. These results indicate that the observed increase in vGAT and GAD65 is not due to increased GABAergic innervation but to increased expression of vGAT and GAD65 in the GABAergic contacts that NL3 or NL2 overexpressing neurons receive. The majority of bright vGAT puncta contacting the NL3 overexpressing neurons have no gephyrin juxtaposed to them indicating that many of these contacts are non-synaptic. This contrasts with the majority of the NL2 overexpressing neurons, which show plenty of synaptic gephyrin clusters juxtaposed to vGAT. Besides having an effect on GABAergic contacts, overexpression of NL3 interferes with the neuronal radial migration, in the cerebral cortex, of the neurons overexpressing NL3.

Keywords

In utero electroporation; glutamic acid decarboxylase; gephyrin; vesicular GABA transporter; synapse formation; neuronal migration; AB_477329; AB_887718; AB_887869; AB_887873;

Corresponding author: Angel L. De Blas, Ph.D., University of Connecticut, Department of Physiology and Neurobiology, 75 North Eagleville Road, U-3156, Storrs, Connecticut, 06269-3156, USA, Tel: (860) 486-5440, Fax: (860) 486-5439, angel.deblas@uconn.edu.

CONFLICT OF INTEREST

The authors declare no financial conflicts of interest.

ROLE OF AUTHORS

Study concept and design: A.L.D. and J.J.L. Acquisition of data: C.F., T-T.C, C.P.M., R.H. and C.G.F. Analysis and interpretation of data: C.F., T-T.C, C.P.M., R.H., C.G.F., J.J.L. and A.L.D. Drafting of the manuscript: A.L.D. Critical revision of the manuscript for important intellectual content: C.F., C.P.M., J.J.L. and A.L.D. Statistical analysis: C.F. and A.L.D. Obtained funding: A.L.D. and J.J.L. Study supervision: C.P.M. and A.L.D.

AB_1279448; AB_2261231; AB_2314493; AB_2314499; AB_2301751; AB_2314477; AB_10063630; nif-0000-30467; nlx_156835; rid_000102

INTRODUCTION

Neuroligins (NLs) are postsynaptic cell-adhesion membrane proteins that trans-synaptically interact with presynaptic neurexins (Ichtchenko et al., 1996). Rodents and humans have four neuroligins (NLs1–4). NL1 is selectively localized in excitatory synapses (Song et al., 1999), NL2 in inhibitory synapses (Varoqueaux et al., 2004), and NL4 in glycinergic synapses (Hoon et al., 2011). NL3 is present in both excitatory and inhibitory synapses (Budreck and Scheiffele, 2007). Neuroligins are considered synaptic organizers involved in activity-dependent stabilization of excitatory and inhibitory synapses (Chubykin et al., 2007; Missler et al., 2012; Shen and Scheiffele, 2010; Siddiqui and Craig, 2011). Mutation and deletions in NL genes have been linked to autism spectrum disorders (ASD) and schizophrenia (Bang and Owczarek, 2013; Missler et al., 2012; Shen and Scheiffele, 2010; Sudhof, 2008).

Much of the current knowledge on the synaptic roles of NLs is derived from manipulating the levels of NL expression in the brain (*in vivo*) and in neuronal cultures. Nevertheless, there are significant differences between the results obtained with neuronal cultures *vs. in vivo*. Thus, in acute neuronal culture experiments, overexpression of NLs promoted the formation and maintenance of synapses (Chih et al., 2005; Gerrow et al., 2006; Levinson et al., 2005; Prange et al., 2004). Knocking down NL1, NL2 or NL3 with the corresponding shRNA, significantly reduced the density of both vesicular glutamate transporter 1 (vGlut1) and vesicular GABA transporter (vGAT)-containing puncta (Chih et al., 2005). However, *in vivo* brain studies with NL1–4 knock out mice have shown that NLs are not essential for synapse formation or maintenance (Baudouin et al., 2012; Blundell et al., 2010; Chubykin et al., 2007; Jamain et al., 2008; Kim et al., 2008; Varoqueaux et al., 2006).

In neuronal cultures, postsynaptic overexpression of NL1 or NL2 led to a non-selective increase in the density of both presynaptic vGlut1 and vGAT puncta (Chih et al., 2005; Levinson et al., 2005; Prange et al., 2004). Also, postsynaptic overexpression of NL1 increased both mEPSCs and mIPSCs frequency and amplitude (Levinson et al., 2005). However, *in vivo* overexpression experiments showed more selective effects on GABAergic or glutamatergic synapses, more in agreement with the normal localization of NL1 in glutamatergic and NL2 in GABAergic synapses. Thus, NL1 overexpression in transgenic mice neurons resulted in increased number of asymmetric (glutamatergic) but not symmetric (GABAergic) synapses (Dahlhaus et al., 2010; Hines et al., 2008). In transgenic mice, overexpression of NL2 increased mIPSC frequency without affecting mEPSCs frequency, but the result was not consistent in two different mouse lines (Hines et al., 2008). In adult-born neurons, overexpression of NL1 did not induce precocious synapse formation, although it led to increased amplitude and frequency of sEPSCs but not of sIPSCs (Schnell et al., 2012). Also, overexpression of NL2 in the dorsal hippocampus (HP) by adeno-associated virus (AAV) delivery, resulted in increased GAD65 mRNA with no effect on vGlut1 mRNA (Kohl et al., 2013).

Regarding NL3, the synaptic effects resulting from acute overexpression have been studied in neuronal cultures (Chih et al., 2005) and organotypic slide cultures (Shipman and Nicoll, 2012b). Nevertheless, to the best of our knowledge, there are no studies on chronic NL3 overexpression *in vivo* yet. This gap needs to be filled given the reported different outcomes observed *in vivo vs*. neuronal cultures, after NL1 or NL2 overexpression. Regarding *in vivo* overexpression of NL2, although two mouse transgenic lines have been studied, some results were not consistent in the two transgenic lines (Hines et al., 2008).

In this communication we report differential effects of clonal NL3 or NL2 overexpression on synapses in the rat cerebral cortex after *in utero* electroporation (IUEP). We also show similarities and differences in the results between *in vivo* and in culture after NL3 or NL2 overexpression. The results also indicate that NL3 overexpression impairs the radial neuronal migration of a subpopulation of NL3 overexpressing neurons.

MATERIALS AND METHODS

Animals

The animal protocols were approved by the Institutional Animal Care and Use Committee and followed the National Institutes of Health guidelines. For hippocampal neuronal cultures and *in utero* electroporation, rat embryos of either sex were used.

Antibodies and plasmids

Table 1 summarizes the primary antibodies used in this study.

A rabbit (Rb) antibody to NL3 was custom-made by Covance (Denver, PA) by immunizing a rabbit (Rb) with the synthetic peptide CEAGPPHDTLRLTALPDYT (corresponding to aa 775–793, GenBank NCBI Ref Seq 588163.2, see also Budreck and Scheiffele, 2007) coupled to keyhole limpet hemocyanin via the N-terminus cysteine. The NL3 antibody was affinity-purified on immobilized peptide antigen. The specificity of the anti-NL3 antibody was demonstrated by 1) sequence specificity of the antigenic peptide as determined from Entrez and UniProt protein databases; 2) enzyme-linked immunosorbent assay (ELISA), which showed binding of anti-NL3 to the antigenic peptide; 3) immunoblots of homogenates and various subcellular fractions from rat forebrain which showed a single 110,000 Mr protein band corresponding to the molecular weight of NL3. The immunoreactivity of the protein band was displaced by antigenic peptide; 4) strong NL3 immunofluorescence signal in human embryonic kidney 293 (HEK293) cells transfected with pCAGGS-HA-NL3 compared to the very low background immunofluorescence signal of neighboring non-transfected cells or HEK293 cells transfected with pCAGGS-HA-NL1 or pCAGGS-HA-NL2; 5) neuronal transfection in culture or *in vivo* with pCAGGS-HA-NL3 showed co-localizing anti-NL3 and anti-HA immunofluorescence signals; 6) neuronal transfection with pCAGGS-HA-NL1 or pCAGGS-HA-NL2 showed anti-HA fluorescence but not anti-NL3 fluorescence.

The Rb antibody to the γ2 subunit of the rat $GABA_AR$ (to amino acids 1–15 QKSDDDYEDYASNKT) was raised and affinity-purified (on immobilized antigen peptide) in our laboratory and has been described and characterized elsewhere (Charych et al., 2004;

Chiou et al., 2011; Christie and De Blas, 2003; Christie et al., 2002a; Christie et al., 2006; Christie et al., 2002b; Jin et al., 2014; Li et al., 2005; Li et al., 2007; Li et al., 2010; Li et al., 2012; Yu and De Blas, 2008; Yu et al., 2007). The RRID is AB_2314477 and it is in the Journal of Comparative Neurology (JCN) antibody database. Triple-label immunofluorescence in cultured hippocampal neurons with this antibody shows clusters that are highly co-localized with the clusters immunolabeled with antibodies to other $GABA_AR$ subunits, such as guinea pig anti-γ2, Rb anti-α1, Rb anti α2, and Ms monoclonal antibody (mAb) anti-β2/3. Immunofluorescence was blocked by the antigenic peptide. In addition, the clusters show apposition to GABAergic presynaptic glutamate decarboxylase (GAD)-containing terminals.

The guinea pig (GP) anti-vGAT (catalog #131004; lot #131004/13; RRID: AB_887873), the Rb anti-vGAT #131003; lot#131003/24; RRID: AB_887869), the mouse (Ms) monoclonal anti-gephyrin (clone mAb7a; catalog #147021; lot lot#147021/9; RRID: AB_1279448) and the Rb anti-gephyrin antibodies (catalog # 147003; lot#147003/20; RRID: AB_887718) were from Synaptic Systems (Gottingen, Germany). These antibodies are in the JCN database.

The Ms Parvalbumin (catalog # P3088; lot#122M4774V; RRID: AB_477329) was from Sigma Aldrich, St. Louis, MO. This antibody is in the JCN database.

The GP anti-vesicular glutamate transporter 1 (vGluT1) of rat vGluT1 (catalog #AB5905; lot# 24080852; RRID: AB_2301751) was from EMD Millipore (Billerica, MA). This antibody is in the JCN antibody database. The Ms anti-HA (catalog #MMS-101R Clone: 16B12; lot#E11EF01029, RRID: AB_10063630) was from Covance. The Rb anti-CDP/cut-like homeobox 1 (CUX1) (catalog # sc-13024; lot#K0309; RRID: AB_2261231), was from Santa Cruz Biotechnology, Santa Cruz, CA). This antibody is in the JCN antibody database. The sheep (Sh) anti-GAD (lot #1440-4, RRID: AB_2314493) was a gift from Dr. Irwin J. Kopin (NINDS, National Institutes of Health, Bethesda, MD). This antibody recognizes a 65-kDa protein band in rat brain immunoblots. The antibody precipitated GAD from rat brain and detected purified GAD in crossed immunoelectrophoresis (Oertel et al., 1981a; Oertel et al., 1981b). This antibody is in the JCN antibody database. The Ms mAb GAD-6 to GAD65 was collected in our laboratory from a supernatant produced in the laboratory from GAD-6 hybridoma cells obtained from the Developmental Studies Hybridoma Bank of the University of Iowa (catalog # GAD-6; RRID: AB_2314499). This antibody is in the JCN antibody database.

For immunofluorescence in cell cultures, fluorophore-labeled fluorescein isothiocyanate (FITC), DyLight 594, or aminomethylcoumarin (AMCA) species-specific anti-IgG antibodies were made in donkey (JacksonImmunoresearch Laboratories, West Grove, PA). For confocal microscopy the species-specific anti-IgG secondary antibodies were raised in goat and labeled with Alexa Fluor 488, 568 or 647 (Invitrogen, Eugene, OR). For epifluorescence microscopy of brain slices, secondary antibodies were raised in donkey and labeled with Alexa Fluor 488 and 568 (JacksonImmunoresearch Laboratories).

Regarding the plasmids, HA-NL2A (in pCAGGS) and HA-NL3A2 (in pNice) were provided by Prof. Peter Scheiffele (Biozentrum, University of Basel). The mRFP was obtained from Dr. Roger Y. Tsien (University of California, San Diego). We subcloned HA-NL3 and mRFP in pCAGGS and used them in the IUEP experiments.

Hippocampal cultures, transfection and immunofluorescence

Hippocampal (HP) neuronal cultures were prepared according to Higgins and Banker (1998) as described elsewhere (Christie and De Blas, 2003; Christie et al., 2002a; Christie et al., 2006; Christie et al., 2002b). Briefly, dissociated neurons from embryonic day 18 (E18) rat hippocampi (from Sprague Dawley rat embryos of either sex) were plated at 3000–8000 cells per 18 mm diameter glass coverslip and maintained in glial cell conditioned medium. HP neurons (10 DIV) were transfected with 2 μg of pCAGGS- HA-NL3 or pCAGGS- HA-NL2 plasmid DNA using the CalPhos mammalian transfection kit (BD Biosciences), following the instructions of the manufacturer. Three days after transfection, cells were subjected to immunofluorescence as described elsewhere (Chiou et al., 2011; Christie et al., 2002a; Christie et al., 2006; Christie et al., 2002b; Li et al., 2009; Li et al., 2010; Li et al., 2012). Briefly, neurons on glass coverslips were fixed in 4% paraformaldehyde, 4% sucrose in phosphate-buffered saline (PBS) for 15 min at room temperature (RT) followed by incubation with 50 mM NH4Cl in PBS for 10–15 minutes. Neurons were permeabilized with 0.25% Triton X-100 in PBS for 5 minutes, followed by 5% donkey normal serum (DNS) in PBS for 30 minutes. The coverslips were then incubated overnight at 4 oC with a mixture of primary antibodies from different species in 0.25% Triton X-100/PBS, followed by incubation with a mixture of fluorophore-conjugated species-specific anti-IgG secondary antibodies in 0.25% Triton X-100/PBS at RT for 1 hour. The coverslips were washed and mounted on glass slides with Prolong Gold antifade mounting solution (Invitrogen, Eugene, OR).

In utero electroporation (IUEP) and immunofluorescence of brain sections

Embryonic rat brain gene transfer by *in utero* electroporation was done as described elsewhere (Li et al., 2005; Li et al., 2010). Briefly, pregnant Wistar rats at 14 days of gestation were anesthetized (with 60 mg/kg ketamine-HCl, 8 mg/kg xylazine, 2 mg/kg acepromazine maleate), and a laparotomy was performed. The uterine horns were gently pulled out and 1–3 μl of a sterile mixture of 0.5 μg/μl of pCAGGS mRFP, pCAGGS-HA-NL3 (or pcAGGS-HA-NL2) and fast green (2 mg/ml; Sigma) were microinjected by pressure with a picospritzer through the uterine wall into the lateral ventricles of the embryos of either sex with a sterile glass capillary pipette. Electroporation was carried out by a brief (1–2 msec) discharge of a 500-μF capacitor charged to 50–100 V. The voltage pulse was discharged with a pair of sterile gold/copper alloy oval plates (1 × 0.5 cm) after gently pinching the head of each embryo through the uterus. After electroporation, the uterus was returned to the abdominal cavity, and the incision was closed by sewing it up with sterile surgical suture.

At P36–40 (for NL3 and NL2) and at P30–31 (for mRFP), the IUEP rats were anesthetized as described above and perfused through the ascending aorta with PB (27 mM NaH2PO4, 92 mM Na2HPO4, pH 7.4) and 4% PLP fixative (4% paraformaldehyde, 1.37% lysine, 0.21%

sodium periodate in 0.1 M phosphate buffer, pH 7.4). Brains were cryoprotected, frozen, and sectioned into 25 μm thick sagittal sections with a freezing microtome. Immunofluorescence of free-floating brain sections has been described elsewhere (Li et al. 2009, 2010). Briefly, brain sections were incubated with 5% normal goat serum (NGS)/0.1 M PB for 1 hour at RT, followed by incubation with a mixture of primary antibodies raised in different species in 2% NGS/0.3% Triton X-100 in PB at 4° C for 2 days. The brain sections were then incubated with a mixture of fluorophore-conjugated species-specific anti-IgG secondary antibodies in 2%NGS/0.3% Triton X-100 in 0.1 M PB at RT for 1 hour and mounted on gelatine-coated glass slides with Prolong Gold anti-fade mounting solution and subjected to laser confocal microscopy.

Image acquisition, analysis, and quantification

Except for the images indicated below, immunofluorescence images of brain slices were acquired on a Leica TCS SP2 laser confocal microscope using a HCX PL Apo ×40/1.25 oil objective lens and a pinhole set at 1 Airy unit. Images were collected with 0.5 μm thick optical sections. For synaptic analysis, images were also collected with a HCXPL Apo 100×/1.4 oil CS objective and 0.1 μm optical sections, with identical results to those obtained with the ×40/1.25 objective. Where indicated, average projections of stacks of consecutive images are presented.

For vGAT and parvalbumin fluorescence quantification (Fig 4), images were collected from cortical layers 2 and 3 in tissue slices and maximal projections of stacks of 5 consecutive images (each 0.5 μm thick) were made in Image J software (NIH, Bethesda, MD, RRID: nif-0000-30467) and a selection area was manually drawn around each cell using the VGAT and Parvalbumin puncta surrounding the cell as guides. A second line was created 10 pixels inside the first line, establishing a 10 pixel wide band between the two lines encompassing the outer surface of the cell. The mean gray value of this area was then calculated for the transfected and non-transfected cells in each image using Image J software. The mean gray value (mean fluorescence intensity/pixel) is the sum of the pixel intensities within the selected area divided by the number of pixels in that area. Statistical analysis of the values calculated by Image J software was performed with InStat 3 (Graphpad in San Diego, CA, RRID: nlx_156835). For Fig 4, a paired t test was used for statistical analysis to match transfected and non-transfected cells from the same image in order to eliminate any variability in background fluorescence between brain sections, animals and experiments. For vGAT, 38 NL3- and 36 NL2-overexpressing neurons and the same number of the corresponding sister non-transfected neurons were analyzed. For parvalbumin, 20 NL3- and 18-NL2-overexpressing neurons and the same number of the corresponding sister non-transfected neurons were analyzed. Data were collected from 2 NL3-and 3 NL2-IUEP brains, from 3–9 brain slices and from 2–4 independent immunofluorescence experiments.

Low magnification fluorescence images of brain sections in Fig 1A and Fig 8A–D, G and H were collected with an epifluorescence Nikon Eclipse 6600 microscope with a Nikon Plan Fluor ×4/0.13 objective (Fig 8A–C, G, H), or a Nikon Plan Fluor ×10/0.3 objective (Fig 1A and Fig 8D), and a Nikon DXM1200 camera driven by Nikon ACT-1 Imaging Software. For Fig 9, values for NL3 were calculated from 7 brain slices (n=7) from two IUEP brains, NL2

from 6 six brain slices (n=6) from two IUEP brains, mRFP from 6 brain slices (n=6) from two IUEP brains. The total number of transfected cells counted for each of the three conditions averaged 1,279±328 (mean ± SEM). The values for the CUX1-labeled non-transfected neurons were calculated from 8 brain slices (n=8) collected from 6 brains, two of each of the transfected with NL3, NL2 or mRFP. The total number of counted CUX1+ non-transfected cells was 3,568. The significance test was ANOVA Tukey-Kramer multiple comparisons test.

Fluorescence images of neuronal cultures were collected using a Nikon Plan Apo ×60/1.40 objective on an Eclipse T300 microscope (Nikon Instruments) with a Photometrics CoolSnap HQ2 CCD camera, driven by IPLab 4.0 (Scanalytics, Rockville, MD, RRID: rid_000102) acquisition software. For qualitative analysis, images were processed and merged for color colocalization in Photoshop CS5 (Adobe, San Jose, CA), adjusting brightness and contrast as described elsewhere (Christie et al., 2002a,b).

RESULTS

Many neuronal precursors that have been *in utero* electroporated with NL3, migrate to the appropriate cortical layers and differentiate into adult neurons that overexpress NL3

Many of the neuronal precursors lining the wall of the ventricle, which were co-transfected with HA-NL3 and mRFP at E14 by IUEP migrated radially to layers II–III of the cerebral cortex (Fig 1A), as shown by mRFP fluorescence (red color). The transfected neurons that have migrated to layers II and III show the normal morphology of differentiated neurons with prominent dendritic arbor, basal dendrites and an apical dendrite that is orientated perpendicular to the pial surface (Fig 1A). The large majority (over 95%) of the mRFP-expressing neurons also express HA-NL3, as shown by double-label immunofluorescence with anti-HA (Fig 1 B). There is also a very good correlation between the expression levels of mRFP and HA-NL3, as shown by the strength of the two fluorescence signals. Neurons that show strong expression of mRFP also show strong co-expression of HA-NL3 (Fig 1B, arrow), while neurons that show weaker expression of mRFP also show weaker co-expression of HA-NL3 (Fig 1B, arrowheads). Triple-label fluorescence experiments (Fig 1C) showed that the mRFP expressing neurons (red) were specifically and strongly labeled with both the anti-HA antibody (green) and the anti-NL3 antibody (blue). NL3 and HA immunofluorescence was clearly observed in the soma and dendrites, both dendritic shafts and dendritic spines, of the transfected neurons (Fig 1D). Axons of transfected neurons also showed HA immunofluorescence (not shown). In control animals in which mRFP were IUEP without HA-NL3, neurons expressing mRFP did not show immunofluorescence signal with the anti-HA or anti-NL3 antibodies (not shown). It is worth mentioning that a high proportion of the HA-NL3 (and mRFP) transfected neurons failed to migrate to layers II–III, which will be discussed below. This contrasts with rats that were IUEP with HA-NL2 and mRFP, where the large majority of the transfected neurons migrated to layers II–III of the cerebral cortex; this will be shown (Fig 8C) and discussed below.

The levels of vGAT are highly and selectively increased in the contacts that NL3-overexpressing neurons receive

Neurons overexpressing mRFP and HA-NL3 showed a very large increase in the extent of vGAT immunofluorescence from the GABAergic contacts that the transfected neurons receive, compared with neighbor non-transfected neurons (Fig 2A–C). 100 % of neurons overexpressing HA-NL3 showed increased extent of vGAT immunofluorescence on their surface. The anti-HA immunofluorescence (blue) co-localized with the mRFP fluorescence (red) ensuring that the increase in vGAT immunofluorescence (green) corresponded to the neurons that overexpressed HA-NL3. Neurons from control rats that were IUEP only with mRFP (without HA-NL3) did not show increase in vGAT immunofluorescence on their surface (Fig 6C1 and C2).

In similar experiments, only 36% of the neurons overexpressing HA-NL2 and mRFP, showed increased vGAT immunofluorescence (green) in their soma and dendrites over neighbor non-transfected neurons (Fig 2D). This increase was considerably smaller than in neurons overexpressing HA-NL3. Moreover, many neurons overexpressing HA-NL2 (blue) did not show increased vGAT immunofluorescence on their surface (Fig 2E). In addition to increased extent of vGAT immunofluorescence, quantification (Fig 4) showed that the mean fluorescence intensity per pixel was also significantly increased in the GABAergic contacts that the HA-NL3 or HA-NL2 overexpressing neurons receive, when compared to the corresponding neighboring non-transfected neurons (for each $p < 0.001$). Note that the effect is considerably stronger for the HA-NL3 (138.6±5.5%) than for the HA-NL2 (111.5±3.0%) overexpressing neurons compared to their respective non-transfected sister neurons (100±3.1% and 100±2.2%). Values are mean ± SEM. Significance was calculated in a paired t test comparing transfected and non-transfected cells from the same image as described in the methods section.

Overexpression of either HA-NL3 (Fig 2F) or HA-NL2 (Fig 2G) did not affect vGlut1 fluorescence extent or intensity in the glutamatergic contacts that the overexpressing neurons receive, compared to either sister non-transfected neurons or neurons overexpressing only mRFP, as determined from animals which were *in utero* electroporated only with mRFP (not shown).

The results show that NL3 or NL2 overexpression in individual brain neurons after IUEP leads to a selective increase in vGAT in the GABAergic contacts but has no effect on vGlut1 in the glutamatergic contacts that innervate the transfected neurons.

The extent of innervation of neurons overexpressing NL3 by parvalbumin-containing GABAergic boutons is not significantly affected

We tested if the increase in vGAT fluorescence observed on the surface of HA-NL3 overexpressing neurons was accompanied by an increase in parvalbumin, a protein marker of a subset of GABAergic interneurons. Parvalbumin concentrates in the presynaptic boutons from these neurons. We used an anti-parvalbumin and an anti-vGAT antibody in triple-label experiments. Fig 3 A and B show that while a transfected neuron (neuron 1) overexpressing HA-NL3 (red) has increased vGAT immunofluorescence (green) on the

surface of its soma, the same neuron showed no apparent increase in parvalbumin (blue) immunofluorescence (either in extent or intensity) over neighboring non-transfected neurons. For instance, non-transfected neurons 2 and 3 of Fig 3A and B that have low vGAT fluorescence, have higher parvalbumin fluorescence intensity than the HA-NL3 overexpressing neuron 1.

In the HA-NL3-transfected neurons there is a perfect match between vGAT and parvalbumin in many presynaptic boutons (Fig 3 A–F, arrowheads), indicating that the vGAT increase can occur in parvalbumin-containing boutons that show no parvalbumin increase. Nevertheless, there are HA-NL3-transfected neurons that show increased vGAT but do not have parvalbumin innervation (Fig 3 G–I) indicating that GABAergic terminals from both parvalbumin and non-parvalbumin interneurons show increased vGAT on their contacts on NL3-overexpressing neurons.

As for HA-NL3, the HA-NL2 overexpressing neurons that show increased vGAT fluorescence, do not show increased parvalbumin fluorescence over non-transfected neurons (Fig 3 J–L, neuron 7 vs. 8 or 9). Quantification (Fig 4) shows that there is no significant difference in parvalbumin fluorescence intensity per pixel in neurons overexpressing NL3 (105.4±8.2; p=0.37) or NL2 (96.2±6.9%; p=0.58) over the corresponding neighboring non-transfected neurons (100±5.4% or 100±5.5% respectively).

Neurons overexpressing NL3 and NL2 also show increased GAD65 immunofluorescence in the GABAergic contacts that these neurons receive

We tested if the increase in vGAT fluorescence on the surface of the HA-NL3 and HA-NL2 overexpressing neurons was accompanied by a significant increase in the GABA-synthesizing enzyme GAD65 in the GABAergic contacts that these neurons receive. Fig 5A and B show that the HA-NL3 and mRFP co-overexpressing neurons have increased GAD65 fluorescence on their surface compared to the non-transfected neighboring neurons. Fig 5C–E shows an example illustrating a neuron co-overexpressing HA-NL2 and mRFP showing increased GAD65 immunofluorescence on its surface. The same neuron also shows increased vGAT immunofluorescence that co-localizes with GAD65 in the GABAergic contacts that the neuron receives.

The neurons overexpressing NL3 frequently do not show gephyrin clusters juxtaposed to the vGAT accumulations on their surface

We tested if the high increase in presynaptic vGAT was accompanied by increases in the GABAergic postsynaptic marker gephyrin. Fig 6A and B show that in NL3-overexpressing neurons, the increase in presynaptic vGAT (green) is not accompanied by an increase in postsynaptic gephyrin cluster number or size (blue) either in the soma (Fig 6 A3–A4) or in the dendrites (Fig 6 A5 and A6). Instead, much of the strong vGAT fluorescence is devoid of associated postsynaptic gephyrin clusters (Fig 6 A3–A6) indicating that many of these contacts are non-synaptic. Moreover, there is an apparent reduction in the size and number of the gephyrin clusters juxtaposed to these contacts compared with sister non-transfected neurons (Fig 6 A1, A2, B1, B2 neurons with asterisk) or control transfected neurons from animals IUEP with only mRFP, without HA-NL3 (Fig 6 C1 and C2, red) or non-transfected

neurons from control animals (Fig 6 C1 and C2, neuron with asterisk). These three types of control neurons show plenty of gephyrin clusters that are juxtaposed to presynaptic vGAT in the soma and dendrites (Fig 6 A1, A2, B1, B2, C1, C2, arrowheads). Also neurons overexpressing HA-NL2 that showed strong vGAT immunofluorescence at their surface, showed frequent juxtaposition of gephyrin clusters to vGAT (Fig 6, D1 and D2, arrowheads). This result contrasted with the highly reduced juxtaposition of gephyrin clusters to vGAT on the surface of NL3-overexpressing neurons.

We also tried to determine if HA-NL3 or HA-NL2, in the corresponding overexpressing neurons, accumulated post-synaptically at GABAergic synapses (Fig 6 E1 and E2, for NL3). The high expression levels of HA-NL3 or HA-NL2 in the transfected neurons precluded determining if there was accumulation of the overexpressed NL at GABAergic contacts. However, neuronal cultures revealed that while HA-NL2 accumulated at GABAergic synapses, HA-NL3 did not (see below).

In neuronal cultures, and in contrast to NL2-overexpressing neurons, the neurons that overexpress NL3 frequently do not show gephyrin or γ2-GABA$_A$R clusters juxtaposed to the GAD accumulations

We also tested if the reduction in gephyrin clusters juxtaposed to GABAergic contacts observed in the HA-NL3 overexpressing neurons in the brain also occurred in neuronal cultures. We have found that many of the GAD boutons contacting the HA-NL3 overexpressing neuron did not have corresponding juxtaposed postsynaptic gephyrin clusters (Fig 7 A1–A4, arrowheads), or γ2-GABA$_A$R clusters (Fig 7C, arrowheads). This was the case in both dendrites (Fig 7 A1–A4, C) and soma (Fig 7 B1–B3). Nevertheless, in HA-NL3 transfected neurons there were also GAD-containing boutons that had juxtaposed gephyrin (Fig 7 A1–A4, arrows) or γ2-GABA$_A$R clusters (Fig 7C, arrows), although these clusters were rather small in size (Fig 7 A1, B2 and C).

Regarding neurons overexpressing HA-NL2, we found that in contrast to neurons overexpressing HA-NL3, the large majority of GAD-containing boutons had robust juxtaposed gephyrin clusters (Fig7 D1–D3, arrows) or γ2-GABA$_A$R clusters (not shown). These results are in agreement with our HA-NL2 overexpression results in the brain. They also show differential synaptic effects of overexpressing NL3 vs NL2 in neurons.

Another difference between HA-NL3 and HA-NL2 in overexpressing cultured HP neurons is that HA-NL3 did not target to GABAergic synapses (Fig 7 A3, red) while HA-NL2 did. Thus, HA-NL2 formed postsynaptic HA-NL2 clusters juxtaposed to GAD-containing boutons, co-localizing with gephyrin clusters. (Fig 7 D2, red, arrows).

At the cell surface NL3 and other NLs prevalently form homodimers and heterodimers (Poulopoulos et al., 2012; Shipman and Nicoll, 2012a). Our results indicate that while NL2 homodimers target to GABAergic synapses, the HA-NL3 homodimers do not target to GABAergic synapses. Nevertheless, the results don't rule out the formation of exogenous HA-NL3 heterodimers with endogenous NL2 that might target to GABAergic synapses. It has been proposed that NL3 forms heterodimers with NL2 at inhibitory synapses (Budreck and Scheiffele, 2007; Kang et al., 2014; Shipman and Nicoll, 2012b). The high expression of

HA-NL3 in transfected neurons precludes the visualization of possible heterodimers of overexpressed HA-NL3 with endogenous NL2.

A large proportion of neurons that overexpress NL3 show impaired radial migration failing to migrate to the upper layers of the cerebral cortex. The misplaced neurons also show increased vGAT in the GABAergic contacts that these cells receive

We have observed that although many HA-NL3 (and mRFP) co-overexpressing neurons, that have been transfected at E14 by IUEP, migrate to the upper layers (II and III) of the cerebral cortex, the majority remain in the lower layers (layers V, VI and white matter), where they extend dendrites (Fig 8 A and B). In contrast, the majority of cells overexpressing HA-NL2 (and mRFP, Fig 8C) or mRFP only (not shown), the latter in control animals IUEP with mRFP only, migrate to the upper layers.

Quantification (Fig 9) shows that a high proportion (73.4±3.3%) of the HA-NL3 (and mRFP) co-overexpressing neurons were present in the lower layers of the cerebral cortex (layers V, VI and white matter). This number was significantly higher than 13.7±1.9% ($p<0.001$) for neurons co-overexpressing HA-NL2 (and mRFP) and 3.2±1.0% ($p<0.001$) for neurons overexpressing mRFP only, which were present in the lower layers of the cerebral cortex. The statistical significance analysis was ANOVA Tukey-Kramer multiple comparisons test. These results suggest that the high percentage of NL3 overexpressing neurons that are present in the lower layers of the cerebral cortex are neurons with impaired radial migration, which have failed to migrate to layers II–III of the cerebral cortex. The results also suggest that NL2 overexpression slightly interferes with neuronal radial migration when compared to mRFP only overexpressing neurons ($p<0.05$ ANOVA). Nevertheless, the large majority of the NL2-overexpressing neurons migrated to layers II and III as the neurons transfected with mRFP only did.

To test the hypothesis that NL3 overexpression impairs radial migration, we did immunofluorescence of the IUEP tissue with CUX1 (CDP/cut-like homeobox1), a transcription factor that is specifically expressed in layers II–IV of the cerebral cortex (Molyneaux et al., 2007; Nieto et al., 2004). As expected, HA-NL3 and mRFP co-overexpressing neurons localized in layers II and III were CUX1+ (Fig 8D). Moreover, 96.3±3.7% of the HA-NL3 and mRFP co-overexpressing neurons that were localized in the lower layers of the cerebral cortex, also expressed CUX1 (Fig 8D, arrowheads) supporting the notion that these are neurons that failed to migrate to layers II– III. Many of the HA-NL2 (and RFP) co-overexpressing neurons or the mRFP-overexpressing neurons that were present in layers V, VI and white matter, also showed expression of CUX1, suggesting that these neurons have also failed to migrate to layers II and III (Fig 8G and H, arrowheads). Moreover, there are also non-transfected neurons expressing CUX1 in the lower layers (Fig 8D and G) of IUEP animals. They likely represent a population of neurons, destined to layers II–IV, which during the normal development of the cerebral cortex fail to migrate to these layers. This notion is supported by the presence of CUX1 expressing neurons in the lower layers of control brains that were not subjected to IUEP (see below). Quantification shows that in the IUEP tissue, 7.5±1.1% of the non-transfected but CUX1-expressing neurons, remained in the lower layers (Fig 9, CUX1-A). In brains of rats not subjected to

IUEP, 8.1±0.3% of the CUX1-expressing neurons remained in the lower layers (Fig 9, CUX1-B). These values were not significantly different from the 3.2±1.0% ($p>0.05$ ANOVA) of mRFP only overexpressing neurons that remained in the lower layers. Thus mRFP overexpression does not significantly alter the normal distribution of CUX1 expressing neurons in the various layers of the cerebral cortex, indicating that mRFP overexpression by itself does not affect normal radial migration of the cortical neurons.

The NL3-overexpressing neurons with impaired radial migration that remained in the lower layers of the cerebral cortex showed increased vGAT immunofluorescence in the contacting GABAergic terminals, when compared to the neighboring non-transfected neurons, as shown in Fig 8F. These neurons also expressed CUX1 (Fig 8E and F). Thus, the neurons overexpressing NL3 in the lower layers showed high vGAT immunofluorescence on their GABAergic surface contacts, similar to the NL3-overexpressing neurons that migrated to layers II–III.

DISCUSSION

In this communication, we have studied the effect of clonal overexpression of NL3 and NL2 in neurons of the rat cerebral cortex *in vivo* after IUEP. To the best of our knowledge, these are the first studies on clonal overexpression of NL3 and NL2 by IUEP and the first studies of NL3 overexpression in the brain. We have found that overexpression of NL3 has strong effects on GABAergic synapses and neuronal radial migration.

Effects on vGAT and GAD65

There is a large increase in vGAT and GAD65 in the GABAergic contacts that the NL3 overexpressing neurons receive. This effect is selective, since there is no effect on the glutamatergic vGlut1. Similar results were obtained after we overexpressed NL2, although the increase in vGAT occurred in a considerably smaller proportion of the NL2 overexpressing neurons and, in the neurons that showed the effect, the increase in vGAT was significantly smaller than in NL3-overexpressing neurons. This selectivity is not found in cultured neurons overexpressing NL3 or NL2, which leads to an increased density of both presynaptic vGAT and vGlut1 puncta (Chih et al., 2005). Also in organotypic slide cultures, overexpression of NL3 increases both glutamatergic and GABAergic synapses (Shipman and Nicoll, 2012b). Increase in both vGAT and vGlut1 fluorescence has also been observed in GABAergic and glutamatergic axons respectively that contact non-neuronal cells overexpressing NL2 in mixed cultures (Graf et al., 2004). Therefore, in the brain, and under our experimental conditions, there are mechanisms that are absent in neuronal cultures that lead to a selective effect of NL3 or NL2 overexpression on GABAergic contacts.

This observed difference in selectivity between IUEP and neuronal culture experiments cannot be attributed to the use of different NL3 or NL2 isoforms derived from alternative splicing (Chih et al., 2006; Sudhof, 2008). The isoforms overexpressed in both neuronal cultures (Chih et al., 2005) and our IUEP experiments were NL3A2 and NL2A.

The selective increase of vGAT *in vivo* after NL2 overexpression is consistent with the selective localization of NL2 at GABAergic synapses in the brain (Varoqueaux et al., 2004)

and with the notion that postsynaptic NL2 is the major player in the selective matching between presynaptic GABAergic boutons and GABAergic post-synapses (Poulopoulos et al., 2009; Soykan et al., 2014). Nevertheless, we find that overexpression of NL3, which is localized in both excitatory and inhibitory synapses (Budreck and Scheiffele, 2007), also induces a selective increase in vGAT, even more than overexpressing NL2, without affecting vGlut1.

Effect on parvalbumin terminals

We have found that chronic overexpression of NL3, and to a lesser extent NL2, highly increased vGAT without significantly affecting the levels of parvalbumin, even in the GABAergic terminals that were double-labeled with vGAT and parvalbumin. It neither increased nor decreased the extent of parvalbumin innervation. These results strongly suggest that the observed increase in vGAT fluorescence extent and intensity, transcellularly induced by NL3 overexpression, was not due to increased GABAergic innervation or increased GABAergic synaptic contacts. Since vGAT is an inhibitory synaptic vesicle marker, the results strongly suggest that NL3 overexpression trans-cellularly induces an increased number of vGAT-containing GABAergic synaptic vesicles in the existing differentiated GABAergic presynaptic contacts as well as in the non-synaptic axonal contacts. Moreover, we have also found that in the NL3-overexpressing neurons, vGAT immunofluorescence frequently did not show juxtaposed postsynaptic gephyrin or $GABA_AR$ clusters *in vivo* and in culture. These results argue against a synaptogenic role of NLs, a notion mainly derived from the interpretation of the results in neuronal cultures. *In vivo* results with NL KO mice have not supported a synaptogenic role for NLs (Varoqueaux et al., 2006). However, it has been shown that NL1 and NL2 are involved in synapse maturation and validation via an activity-dependent mechanism (Chubykin et al., 2007; Kwon et al., 2012; Varoqueaux et al., 2006). It is not known if NL3 is involved in synapse maturation and validation. Contrary to NL1 (Kwon et al., 2012; Shipman and Nicoll, 2012b), NL3 is not involved in LTP (Shipman and Nicoll, 2012b).

We have found that the increase in vGAT fluorescence in the GABAergic contacts present on the surface of NL3- or NL2-overexpressing neurons was accompanied by increased GAD65 fluorescence, indicating that both NLs induce a trans-cellular coordinated increase in both vGAT and the GABA-synthesizing enzyme GAD65. These results strongly suggest that in these contacts, there is increased GABA synthesis and storage in an increased number of GABAergic synaptic vesicles, compared to that of the GABAergic contacts on the surface of non-transfected neurons. Because NLs trans-synaptically interact with presynaptic neurexins and the latter recruit voltage-gated Ca^{2+} channels and components of the neurotransmitter release machinery (Biederer and Sudhof, 2000; Biederer and Sudhof, 2001; Hata et al., 1996; Missler et al., 2003), it is likely that the GABAergic contacts surrounding the NL3- or NL2- overexpressing neurons release high quantities of GABA upon membrane depolarization. This could result in increased phasic and/or tonic inhibition of these NL-overexpressing neurons via synaptic and/or extrasynaptic $GABA_ARs$ respectively.

Postsynaptic effects

There are also important postsynaptic differences between NL3 and NL2 overexpressing neurons. I*n vivo* and in culture, most of the vGAT innervating NL3-overexpressing neurons showed no juxtaposed gephyrin clusters, indicating that the majority of these contacts are non-synaptic. In contrast, the majority of the vGAT innervation of the NL2-overexpressing neurons had juxtaposed gephyrin clusters. A possible explanation for this difference is that overexpression of NL3 could disrupt the direct interaction of endogenous NL2 with postsynaptic gephyrin or collybistin at the GABAergic postsynapse (*i.e*. by HA-NL3 forming heterodimers with endogenous NL2). Thus, although the cytoplasmic domain of all neuroligins have a gephyrin-binding domain (Poulopoulos et al., 2009; Soykan et al., 2014), only NL2 and NL4 have the collybistin-binding domain that presumably is involved in collybistin activation and the nucleation of gephyrin clustering at the postsynapse (Poulopoulos et al., 2009; Soykan et al., 2014). Another possibility is that overexpression of NL3 in the postsynaptic neuron could displace the trans-synaptic interactions of presynaptic neurexins with a variety of postsynaptic neurexin-binding partners, which are known to be involved in synapse stabilization and maturation, thus disrupting postsynaptic gephyrin clustering. Known NRXN trans-synaptic interacting partners are leucine-rich repeat transmembrane neuronal proteins LRRTMs (de Wit et al., 2009; Ko et al., 2009; Linhoff et al., 2009; Siddiqui et al., 2010), Calsyntenin-3 (Pettem et al., 2013a), receptor-type protein tyrosine phosphatases PTPRT (Kwon et al., 2010; Woo et al., 2009), the complex cerebellin1-GluR™2 (Matsuda et al., 2010; Uemura et al., 2010), dystroglycans (Reissner et al., 2014; Sugita et al., 2001) and neurexophilins (Missler et al., 1998; Missler and Sudhof, 1998). Another possibility is that the down-regulation of gephyrin and the postsynaptic element is a compensatory mechanism to the up-regulation of vGAT and GAD and the presumed increase in GABA release.

Regarding NL2, two transgenic mouse lines have been developed and studied by the same group with different line-dependent results (Hines et al., 2008). There is an increase in vGAT but not gephyrin, an increase in the frequency but not amplitude of mIPSCs, no change in mEPSCs, a preferential increase in the number of symmetric over asymmetric synapses and an increase in the number of synaptic vesicles in the reserve pool. These results in transgenic mice are consistent with our NL2 overexpression studies by IUEP. Nevertheless, some of the observed changes in the NL2 transgenes were line-dependent (Hines et al., 2008), which underscores the value of the IUEP approach for *in vivo* studies. Moreover, it has been shown that manipulation of NL1 after IUEP can unveil phenotypes different from those observed after genetic manipulation of animal models (Kwon et al., 2012).

It is worth mentioning that our *in vivo* NL3 and NL2 overexpression studies were done in rat while the aforementioned *in vivo* overexpression studies of NL2 were done in mouse.

Effects on radial neuronal migration

Our results are also consistent with the notion that NL3 overexpression impairs the radial migration of a significant number of neurons to the upper layers of the cerebral cortex. To the best of our knowledge, this effect of NL3 overexpression on neuronal radial migration

has not been previously reported. It has been shown that NL-NRXN interaction slows down cell migration in vitro (Pautot et al., 2005) and therefore, it is conceivable that the overexpression of NL3 in some migrating neurons enhances the interaction with NRXs from the radial glia, slowing down radial migration. Nevertheless, it does not seem to be a general mechanism for all NLs, since overexpression of NL2 shows a considerably milder effect on neuronal migration, as we have shown above.

The cell adhesion molecule MDGA1 is involved in radial neuronal migration in a subset of cortical neurons (Ishikawa et al., 2011) and the knockout of MDGA1 produces a mild neuronal migration phenotype (Ishikawa et al., 2011). MDGA1 and MDGA2 cis-interact with NL2, blocking the trans-interaction of NL2 with NRXNs (Lee et al., 2013; Pettem et al., 2013b). Nevertheless, it is unlikely that MDGA1 (or MDGA2) are involved in the radial migration phenotype resulting from NL3 overexpression, since MDGA1 and MDGA2 do not interact with NL3 (or NL1) and the migration phenotype of NL2 overexpression is very mild. MDGA1 and MDGA2 also reduce the number of inhibitory synapses, by blocking the interaction of NL2 with NRXNs (Lee et al., 2013; Pettem et al., 2013b).

It has been proposed that GABA, via $GABA_AR$ activation, is an extracellular signal that regulates neuronal migration, promoting or inhibiting migration depending on whether GABA depolarizes or hyperpolarizes the neuron (Behar et al., 2000; Bortone and Polleux, 2009; Maher and LoTurco, 2009; Manent et al., 2005). The increase in vGAT in the GABAergic contacts that the NL3-overexpressing neurons receive in the lower cortical layers could result in increased GABA released by these terminals, followed by the activation of synaptic and extrasynaptic $GABA_ARs$ of the NL3-overexpressing neurons and reduction of their radial migration, perhaps by affecting intracellular Ca^{2+} levels (Komuro and Rakic, 1998; Komuro et al., 2014). If that were the case, the inhibitory effect on migration would be more pronounced on NL3- over NL2-overexpressing neurons, as we have observed, since NL3 induces stronger effect on vGAT up-regulation than NL2, presumably resulting in higher GABA release from the GABAergic contacts innervating the NL3-overexpressing neurons.

It has been shown that impairment of neuronal migration in the cerebral cortex leads to various neurodevelopmental disorders by altering local and long-distance circuits (Liu, 2011; Manent et al., 2011; Manzini and Walsh, 2011). Conceivably, mutations that affect NL3 expression could alter normal neuronal migration and neuronal connectivity, contributing to the autism spectrum disorders (ASD) associated with alterations of NL3 expression (see below).

In vivo clonal overexpression studies

Our results indicate that NL3 overexpression likely alters the balance between excitation and inhibition in the NL3-overexpressing neurons. A prevalent hypothesis is that in ASD, and in some other neurodevelopmental disorders, the balance between excitation and inhibition is altered (Bourgeron, 2009; Zoghbi, 2003). There is an association between NL3 and ASD (Baudouin et al., 2012; Chih et al., 2004; Etherton et al., 2011a; Gilman et al., 2011; Jamain et al., 2003; Sanders et al., 2011; Sudhof, 2008). These include NL3 mutations, such as a R451C and R704C point mutations (Etherton et al., 2011b; Jamain et al., 2003) and

deletions that eliminate NL3 entire sequence (Gilman et al., 2011; Levy et al., 2011; Sanders et al., 2011). These germ line mutations and deletions are transmitted to all cells of the offspring. In our studies, NL3 overexpression does not affect all brain cells. It is restricted to a subpopulation of neurons in the cerebral cortex, distributed in a mosaic-like fashion, which is derived from the electroporation of a population of neuronal precursors, their clonal descendants and their radial migration. This experimental situation would be analogous to what would happen during the development of the cerebral cortex if a somatic mutation or a somatic copy number variation (CNV) would occur in a neuronal precursor, due to the cortical clonal architecture of the cerebral cortex. Clonal somatic mosaic mutations have been linked to brain malformations (Cai et al., 2014; Lee et al., 2012; Poduri et al., 2013). It has been estimated that a small population of neurons (as low as 8–35%) carrying a de novo somatic mutation can affect the function of widespread cortical circuits, leading to neurological disorders (Poduri et al., 2013). It has also been shown that clonal somatic CNVs are abundant in human brain neurons (Cai et al., 2014; McConnell et al., 2013). There is the hope that new single-cell sequencing technologies and approaches will lead to the identification of clonal somatic mutations and CNVs associated with ASD and neurodevelopmental disorders. There is no evidence that clonal overexpression of NL3 might occur in some humans or is associated with any neurodevelopmental disorder. Nevertheless, it is conceivable that a de novo somatic mutation or CNV that results in a loss of function of a NL3 repressor would increase the expression of NL3 in a clone of neurons intermingled with non-mutated clones, forming mosaics in a fashion similar to the IUEP studies. Moreover, NL3 overexpression could also impair the normal radial migration of a subset of neurons affecting their local and long-distance connectivity, altering the balance between excitation and inhibition. Thus clonal overexpression of NL3 or other molecules by IUEP could in certain cases be valuable models in the study of some neurodevelopmental disorders.

OTHER ACKNOWLEDGEMENTS

We thank Prof. Peter Scheiffele (Biozentrum, University of Basel) for providing the NL2 and NL3 plasmids.

Grant support: This research was supported by the NIH/NICHD grant RO1HD055655 to J.J.L. and the NIH-NIND grant R01NS038752 to A.L.D.

ABBREVIATIONS

aa	amino acids
ASD	autism spectrum disorder
CNV	copy number variation
CUX1	cut-like homeobox 1
GABA	γ-aminobutyric acid
$GABA_AR$	γ-aminobutyric acid type A receptor
GAD	glutamic acid decarboxylase
GP	guinea pig

HA	human Influenza hemaglutinin
HP	hippocampus
IUEP	*in utero* electroporation
KO	knockout
LTP	long term potentiation
mAb	monoclonal antibody
MDGA	MAM domain-containing glycosylphosphatidylinositol anchor
mIPSC	miniature inhibitory postsynaptic current
mRFP	monomeric red fluorescent protein
Ms	mouse
NL	neuroligin
NRXN	neurexin
Rb	rabbit
RT	room temperature
sEPSC	spontaneous excitatory postsynaptic current
Sh	sheep
shRNA	short hairpin RNA
sIPSC	spontaneous inhibitory postsynaptic currents
vGAT	vesicular GABA transporter
vGlut1	vesicular glutamate transporter 1

LITERATURE CITED

Bang ML, Owczarek S. A matter of balance: role of neurexin and neuroligin at the synapse. Neurochemical research. 2013; 38:1174–1189. [PubMed: 23559421]

Baudouin SJ, Gaudias J, Gerharz S, Hatstatt L, Zhou K, Punnakkal P, Tanaka KF, Spooren W, Hen R, De Zeeuw CI, Vogt K, Scheiffele P. Shared synaptic pathophysiology in syndromic and nonsyndromic rodent models of autism. Science. 2012; 338:128–132. [PubMed: 22983708]

Behar TN, Schaffner AE, Scott CA, Greene CL, Barker JL. GABA receptor antagonists modulate postmitotic cell migration in slice cultures of embryonic rat cortex. Cerebral cortex. 2000; 10:899–909. [PubMed: 10982750]

Biederer T, Sudhof TC. Mints as adaptors. Direct binding to neurexins and recruitment of munc18. The Journal of biological chemistry. 2000; 275:39803–39806. [PubMed: 11036064]

Biederer T, Sudhof TC. CASK and protein 4.1 support F-actin nucleation on neurexins. The Journal of biological chemistry. 2001; 276:47869–47876. [PubMed: 11604393]

Blundell J, Blaiss CA, Etherton MR, Espinosa F, Tabuchi K, Walz C, Bolliger MF, Sudhof TC, Powell CM. Neuroligin-1 deletion results in impaired spatial memory and increased repetitive behavior. J Neurosci. 2010; 30:2115–2129. [PubMed: 20147539]

Bortone D, Polleux F. KCC2 expression promotes the termination of cortical interneuron migration in a voltage-sensitive calcium-dependent manner. Neuron. 2009; 62:53–71. [PubMed: 19376067]

Bourgeron T. A synaptic trek to autism. Current opinion in neurobiology. 2009; 19:231–234. [PubMed: 19545994]

Budreck EC, Scheiffele P. Neuroligin-3 is a neuronal adhesion protein at GABAergic and glutamatergic synapses. Eur J Neurosci. 2007; 26:1738–1748. [PubMed: 17897391]

Cai X, Evrony GD, Lehmann HS, Elhosary PC, Mehta BK, Poduri A, Walsh CA. Single-Cell, Genome-wide Sequencing Identifies Clonal Somatic Copy-Number Variation in the Human Brain. Cell reports. 2014

Charych EI, Yu W, Li R, Serwanski DR, Miralles CP, Li X, Yang BY, Pinal N, Walikonis R, De Blas AL. A four PDZ domain-containing splice variant form of GRIP1 is localized in GABAergic and glutamatergic synapses in the brain. J Biol Chem. 2004; 279:38978–38990. [PubMed: 15226318]

Chih B, Afridi SK, Clark L, Scheiffele P. Disorder-associated mutations lead to functional inactivation of neuroligins. Hum Mol Genet. 2004; 13:1471–1477. [PubMed: 15150161]

Chih B, Engelman H, Scheiffele P. Control of excitatory and inhibitory synapse formation by neuroligins. Science. 2005; 307:1324–1328. [PubMed: 15681343]

Chih B, Gollan L, Scheiffele P. Alternative splicing controls selective trans-synaptic interactions of the neuroligin-neurexin complex. Neuron. 2006; 51:171–178. [PubMed: 16846852]

Chiou TT, Bonhomme B, Jin H, Miralles CP, Xiao H, Fu Z, Harvey RJ, Harvey K, Vicini S, De Blas AL. Differential regulation of the postsynaptic clustering of gamma-aminobutyric acid type A (GABAA) receptors by collybistin isoforms. J Biol Chem. 2011; 286:22456–22468. [PubMed: 21540179]

Christie SB, De Blas AL. GABAergic and glutamatergic axons innervate the axon initial segment and organize GABA(A) receptor clusters of cultured hippocampal pyramidal cells. J Comp Neurol. 2003; 456:361–374. [PubMed: 12532408]

Christie SB, Li RW, Miralles CP, Riquelme R, Yang BY, Charych E, Wendou Y, Daniels SB, Cantino ME, De Blas AL. Synaptic and extrasynaptic GABAA receptor and gephyrin clusters. Prog Brain Res. 2002a; 136:157–180. [PubMed: 12143379]

Christie SB, Li RW, Miralles CP, Yang BY, De Blas AL. Clustered and non-clustered GABAA receptors in cultured hippocampal neurons. Mol Cell Neurosci. 2006; 31:1–14. [PubMed: 16181787]

Christie SB, Miralles CP, De Blas AL. GABAergic innervation organizes synaptic and extrasynaptic GABAA receptor clustering in cultured hippocampal neurons. J Neurosci. 2002b; 22:684–697. [PubMed: 11826098]

Chubykin AA, Atasoy D, Etherton MR, Brose N, Kavalali ET, Gibson JR, Sudhof TC. Activity-dependent validation of excitatory versus inhibitory synapses by neuroligin-1 versus neuroligin-2. Neuron. 2007; 54:919–931. [PubMed: 17582332]

Dahlhaus R, Hines RM, Eadie BD, Kannangara TS, Hines DJ, Brown CE, Christie BR, El-Husseini A. Overexpression of the cell adhesion protein neuroligin-1 induces learning deficits and impairs synaptic plasticity by altering the ratio of excitation to inhibition in the hippocampus. Hippocampus. 2010; 20:305–322. [PubMed: 19437420]

de Wit J, Sylwestrak E, O'Sullivan ML, Otto S, Tiglio K, Savas JN, Yates JR 3rd, Comoletti D, Taylor P, Ghosh A. LRRTM2 interacts with Neurexin1 and regulates excitatory synapse formation. Neuron. 2009; 64:799–806. [PubMed: 20064388]

Etherton M, Foldy C, Sharma M, Tabuchi K, Liu X, Shamloo M, Malenka RC, Sudhof TC. Autism-linked neuroligin-3 R451C mutation differentially alters hippocampal and cortical synaptic function. Proc Natl Acad Sci U S A. 2011a; 108:13764–13769. [PubMed: 21808020]

Etherton MR, Tabuchi K, Sharma M, Ko J, Sudhof TC. An autism-associated point mutation in the neuroligin cytoplasmic tail selectively impairs AMPA receptor-mediated synaptic transmission in hippocampus. EMBO J. 2011b; 30:2908–2919. [PubMed: 21642956]

Gerrow K, Romorini S, Nabi SM, Colicos MA, Sala C, El-Husseini A. A preformed complex of postsynaptic proteins is involved in excitatory synapse development. Neuron. 2006; 49:547–562. [PubMed: 16476664]

Gilman SR, Iossifov I, Levy D, Ronemus M, Wigler M, Vitkup D. Rare de novo variants associated with autism implicate a large functional network of genes involved in formation and function of synapses. Neuron. 2011; 70:898–907. [PubMed: 21658583]

Graf ER, Zhang X, Jin SX, Linhoff MW, Craig AM. Neurexins induce differentiation of GABA and glutamate postsynaptic specializations via neuroligins. Cell. 2004; 119:1013–1026. [PubMed: 15620359]

Hata Y, Butz S, Sudhof TC. CASK: a novel dlg/PSD95 homolog with an N-terminal calmodulin-dependent protein kinase domain identified by interaction with neurexins. J Neurosci. 1996; 16:2488–2494. [PubMed: 8786425]

Hines RM, Wu L, Hines DJ, Steenland H, Mansour S, Dahlhaus R, Singaraja RR, Cao X, Sammler E, Hormuzdi SG, Zhuo M, El-Husseini A. Synaptic imbalance, stereotypies, and impaired social interactions in mice with altered neuroligin 2 expression. J Neurosci. 2008; 28:6055–6067. [PubMed: 18550748]

Hoon M, Soykan T, Falkenburger B, Hammer M, Patrizi A, Schmidt KF, Sassoe-Pognetto M, Lowel S, Moser T, Taschenberger H, Brose N, Varoqueaux F. Neuroligin-4 is localized to glycinergic postsynapses and regulates inhibition in the retina. Proc Natl Acad Sci U S A. 2011; 108:3053–3058. [PubMed: 21282647]

Ichtchenko K, Nguyen T, Sudhof TC. Structures, alternative splicing, and neurexin binding of multiple neuroligins. The Journal of biological chemistry. 1996; 271:2676–2682. [PubMed: 8576240]

Ishikawa T, Gotoh N, Murayama C, Abe T, Iwashita M, Matsuzaki F, Suzuki T, Yamamoto T. IgSF molecule MDGA1 is involved in radial migration and positioning of a subset of cortical upper-layer neurons. Developmental dynamics : an official publication of the American Association of Anatomists. 2011; 240:96–107. [PubMed: 21104742]

Jamain S, Quach H, Betancur C, Rastam M, Colineaux C, Gillberg IC, Soderstrom H, Giros B, Leboyer M, Gillberg C, Bourgeron T. Paris Autism Research International Sibpair S. Mutations of the X-linked genes encoding neuroligins NLGN3 and NLGN4 are associated with autism. Nature genetics. 2003; 34:27–29. [PubMed: 12669065]

Jamain S, Radyushkin K, Hammerschmidt K, Granon S, Boretius S, Varoqueaux F, Ramanantsoa N, Gallego J, Ronnenberg A, Winter D, Frahm J, Fischer J, Bourgeron T, Ehrenreich H, Brose N. Reduced social interaction and ultrasonic communication in a mouse model of monogenic heritable autism. Proc Natl Acad Sci U S A. 2008; 105:1710–1715. [PubMed: 18227507]

Jin H, Chiou TT, Serwanski DR, Miralles CP, Pinal N, De Blas AL. RNF34 interacts with and promotes gamma-aminobutyric acid type-A receptor degradation via ubiquitination of the gamma2 subunit. J Biol Chem. 2014

Kang Y, Ge Y, Cassidy RM, Lam V, Luo L, Moon KM, Lewis R, Molday RS, Wong RO, Foster LJ, Craig AM. A Combined Transgenic Proteomic Analysis and Regulated Trafficking of Neuroligin-2. The Journal of biological chemistry. 2014

Kim J, Jung SY, Lee YK, Park S, Choi JS, Lee CJ, Kim HS, Choi YB, Scheiffele P, Bailey CH, Kandel ER, Kim JH. Neuroligin-1 is required for normal expression of LTP and associative fear memory in the amygdala of adult animals. Proc Natl Acad Sci U S A. 2008; 105:9087–9092. [PubMed: 18579781]

Ko J, Fuccillo MV, Malenka RC, Sudhof TC. LRRTM2 functions as a neurexin ligand in promoting excitatory synapse formation. Neuron. 2009; 64:791–798. [PubMed: 20064387]

Kohl C, Riccio O, Grosse J, Zanoletti O, Fournier C, Schmidt MV, Sandi C. Hippocampal neuroligin-2 overexpression leads to reduced aggression and inhibited novelty reactivity in rats. PloS one. 2013; 8:e56871. [PubMed: 23451101]

Komuro H, Rakic P. Orchestration of neuronal migration by activity of ion channels, neurotransmitter receptors, and intracellular Ca2+ fluctuations. Journal of neurobiology. 1998; 37:110–130. [PubMed: 9777736]

Komuro Y, Galas L, Lebon A, Raoult E, Fahrion JK, Tilot A, Kumada T, Ohno N, Vaudry D, Komuro H. The role of calcium and cyclic nucleotide signaling in cerebellar granule cell migration under normal and pathological conditions. Developmental neurobiology. 2014 [Epub ahead of print].

Kwon HB, Kozorovitskiy Y, Oh WJ, Peixoto RT, Akhtar N, Saulnier JL, Gu C, Sabatini BL. Neuroligin-1-dependent competition regulates cortical synaptogenesis and synapse number. Nature neuroscience. 2012; 15:1667–1674.

Kwon SK, Woo J, Kim SY, Kim H, Kim E. Trans-synaptic adhesions between netrin-G ligand-3 (NGL-3) and receptor tyrosine phosphatases LAR, protein-tyrosine phosphatase delta (PTPdelta),

and PTPsigma via specific domains regulate excitatory synapse formation. The Journal of biological chemistry. 2010; 285:13966–13978. [PubMed: 20139422]

Lee JH, Huynh M, Silhavy JL, Kim S, Dixon-Salazar T, Heiberg A, Scott E, Bafna V, Hill KJ, Collazo A, Funari V, Russ C, Gabriel SB, Mathern GW, Gleeson JG. De novo somatic mutations in components of the PI3K-AKT3-mTOR pathway cause hemimegalencephaly. Nature genetics. 2012; 44:941–945. [PubMed: 22729223]

Lee K, Kim Y, Lee SJ, Qiang Y, Lee D, Lee HW, Kim H, Je HS, Sudhof TC, Ko J. MDGAs interact selectively with neuroligin-2 but not other neuroligins to regulate inhibitory synapse development. Proc Natl Acad Sci U S A. 2013; 110:336–341. [PubMed: 23248271]

Levinson JN, Chery N, Huang K, Wong TP, Gerrow K, Kang R, Prange O, Wang YT, El-Husseini A. Neuroligins mediate excitatory and inhibitory synapse formation: involvement of PSD-95 and neurexin-1beta in neuroligin-induced synaptic specificity. The Journal of biological chemistry. 2005; 280:17312–17319. [PubMed: 15723836]

Levy D, Ronemus M, Yamrom B, Lee YH, Leotta A, Kendall J, Marks S, Lakshmi B, Pai D, Ye K, Buja A, Krieger A, Yoon S, Troge J, Rodgers L, Iossifov I, Wigler M. Rare de novo and transmitted copy-number variation in autistic spectrum disorders. Neuron. 2011; 70:886–897. [PubMed: 21658582]

Li RW, Yu W, Christie S, Miralles CP, Bai J, Loturco JJ, De Blas AL. Disruption of postsynaptic GABA receptor clusters leads to decreased GABAergic innervation of pyramidal neurons. Journal of neurochemistry. 2005; 95:756–770. [PubMed: 16248887]

Li X, Serwanski DR, Miralles CP, Bahr BA, De Blas AL. Two pools of Triton X-100-insoluble GABA(A) receptors are present in the brain, one associated to lipid rafts and another one to the post-synaptic GABAergic complex. J Neurochem. 2007; 102:1329–1345. [PubMed: 17663755]

Li X, Serwanski DR, Miralles CP, Nagata K, De Blas AL. Septin 11 is present in GABAergic synapses and plays a functional role in the cytoarchitecture of neurons and GABAergic synaptic connectivity. J Biol Chem. 2009; 284:17253–17265. [PubMed: 19380581]

Li Y, Serwanski DR, Miralles CP, Fiondella CG, Loturco JJ, Rubio ME, De Blas AL. Synaptic and nonsynaptic localization of protocadherin-gammaC5 in the rat brain. The Journal of comparative neurology. 2010; 518:3439–3463. [PubMed: 20589908]

Li Y, Xiao H, Chiou TT, Jin H, Bonhomme B, Miralles CP, Pinal N, Ali R, Chen WV, Maniatis T, De Blas AL. Molecular and functional interaction between protocadherin-gammaC5 and GABAA receptors. J Neurosci. 2012; 32:11780–11797. [PubMed: 22915120]

Linhoff MW, Lauren J, Cassidy RM, Dobie FA, Takahashi H, Nygaard HB, Airaksinen MS, Strittmatter SM, Craig AM. An unbiased expression screen for synaptogenic proteins identifies the LRRTM protein family as synaptic organizers. Neuron. 2009; 61:734–749. [PubMed: 19285470]

Liu JS. Molecular genetics of neuronal migration disorders. Current neurology and neuroscience reports. 2011; 11:171–178. [PubMed: 21222180]

Maher BJ, LoTurco JJ. Stop and go GABA. Nature neuroscience. 2009; 12:817–818.

Manent JB, Beguin S, Ganay T, Represa A. Cell-autonomous and cell-to-cell signalling events in normal and altered neuronal migration. Eur J Neurosci. 2011; 34:1595–1608. [PubMed: 22103417]

Manent JB, Demarque M, Jorquera I, Pellegrino C, Ben-Ari Y, Aniksztejn L, Represa A. A noncanonical release of GABA and glutamate modulates neuronal migration. J Neurosci. 2005; 25:4755–4765. [PubMed: 15888651]

Manzini MC, Walsh CA. What disorders of cortical development tell us about the cortex: one plus one does not always make two. Current opinion in genetics & development. 2011; 21:333–339. [PubMed: 21288712]

Matsuda K, Miura E, Miyazaki T, Kakegawa W, Emi K, Narumi S, Fukazawa Y, Ito-Ishida A, Kondo T, Shigemoto R, Watanabe M, Yuzaki M. Cbln1 is a ligand for an orphan glutamate receptor delta2, a bidirectional synapse organizer. Science. 2010; 328:363–368. [PubMed: 20395510]

McConnell MJ, Lindberg MR, Brennand KJ, Piper JC, Voet T, Cowing-Zitron C, Shumilina S, Lasken RS, Vermeesch JR, Hall IM, Gage FH. Mosaic copy number variation in human neurons. Science. 2013; 342:632–637. [PubMed: 24179226]

Missler M, Hammer RE, Sudhof TC. Neurexophilin binding to alpha-neurexins. A single LNS domain functions as an independently folding ligand-binding unit. The Journal of biological chemistry. 1998; 273:34716–34723. [PubMed: 9856994]

Missler M, Sudhof TC. Neurexophilins form a conserved family of neuropeptide-like glycoproteins. J Neurosci. 1998; 18:3630–3638. [PubMed: 9570794]

Missler M, Sudhof TC, Biederer T. Synaptic cell adhesion. Cold Spring Harbor perspectives in biology. 2012; 4:a005694. [PubMed: 22278667]

Missler M, Zhang W, Rohlmann A, Kattenstroth G, Hammer RE, Gottmann K, Sudhof TC. Alpha-neurexins couple Ca2+ channels to synaptic vesicle exocytosis. Nature. 2003; 423:939–948. [PubMed: 12827191]

Molyneaux BJ, Arlotta P, Menezes JR, Macklis JD. Neuronal subtype specification in the cerebral cortex. Nature reviews Neuroscience. 2007; 8:427–437.

Nieto M, Monuki ES, Tang H, Imitola J, Haubst N, Khoury SJ, Cunningham J, Gotz M, Walsh CA. Expression of Cux-1 and Cux-2 in the subventricular zone and upper layers II–IV of the cerebral cortex. The Journal of comparative neurology. 2004; 479:168–180. [PubMed: 15452856]

Oertel WH, Schmechel DE, Mugnaini E, Tappaz ML, Kopin IJ. Immunocytochemical localization of glutamate decarboxylase in rat cerebellum with a new antiserum. Neuroscience. 1981a; 6:2715–2735. [PubMed: 7033824]

Oertel WH, Schmechel DE, Tappaz ML, Kopin IJ. Production of a specific antiserum to rat brain glutamic acid decarboxylase by injection of an antigen-antibody complex. Neuroscience. 1981b; 6:2689–2700. [PubMed: 7322358]

Pautot S, Lee H, Isacoff EY, Groves JT. Neuronal synapse interaction reconstituted between live cells and supported lipid bilayers. Nature chemical biology. 2005; 1:283–289.

Pettem KL, Yokomaku D, Luo L, Linhoff MW, Prasad T, Connor SA, Siddiqui TJ, Kawabe H, Chen F, Zhang L, Rudenko G, Wang YT, Brose N, Craig AM. The specific alpha-neurexin interactor calsyntenin-3 promotes excitatory and inhibitory synapse development. Neuron. 2013a; 80:113–128. [PubMed: 24094106]

Pettem KL, Yokomaku D, Takahashi H, Ge Y, Craig AM. Interaction between autism-linked MDGAs and neuroligins suppresses inhibitory synapse development. J Cell Biol. 2013b; 200:321–336. [PubMed: 23358245]

Poduri A, Evrony GD, Cai X, Walsh CA. Somatic mutation, genomic variation, and neurological disease. Science. 2013; 341:1237758. [PubMed: 23828942]

Poulopoulos A, Aramuni G, Meyer G, Soykan T, Hoon M, Papadopoulos T, Zhang M, Paarmann I, Fuchs C, Harvey K, Jedlicka P, Schwarzacher SW, Betz H, Harvey RJ, Brose N, Zhang W, Varoqueaux F. Neuroligin 2 drives postsynaptic assembly at perisomatic inhibitory synapses through gephyrin and collybistin. Neuron. 2009; 63:628–642. [PubMed: 19755106]

Poulopoulos A, Soykan T, Tuffy LP, Hammer M, Varoqueaux F, Brose N. Homodimerization and isoform-specific heterodimerization of neuroligins. The Biochemical journal. 2012; 446:321–330. [PubMed: 22671294]

Prange O, Wong TP, Gerrow K, Wang YT, El-Husseini A. A balance between excitatory and inhibitory synapses is controlled by PSD-95 and neuroligin. Proc Natl Acad Sci U S A. 2004; 101:13915–13920. [PubMed: 15358863]

Reissner C, Stahn J, Breuer D, Klose M, Pohlentz G, Mormann M, Missler M. Dystroglycan Binding to alpha-Neurexin Competes with Neurexophilin-1 and Neuroligin in the Brain. The Journal of biological chemistry. 2014

Sanders SJ, Ercan-Sencicek AG, Hus V, Luo R, Murtha MT, Moreno-De-Luca D, Chu SH, Moreau MP, Gupta AR, Thomson SA, Mason CE, Bilguvar K, Celestino-Soper PB, Choi M, Crawford EL, Davis L, Wright NR, Dhodapkar RM, DiCola M, DiLullo NM, Fernandez TV, Fielding-Singh V, Fishman DO, Frahm S, Garagaloyan R, Goh GS, Kammela S, Klei L, Lowe JK, Lund SC, McGrew AD, Meyer KA, Moffat WJ, Murdoch JD, O'Roak BJ, Ober GT, Pottenger RS, Raubeson MJ, Song Y, Wang Q, Yaspan BL, Yu TW, Yurkiewicz IR, Beaudet AL, Cantor RM, Curland M, Grice DE, Gunel M, Lifton RP, Mane SM, Martin DM, Shaw CA, Sheldon M, Tischfield JA, Walsh CA, Morrow EM, Ledbetter DH, Fombonne E, Lord C, Martin CL, Brooks AI, Sutcliffe JS, Cook EH Jr, Geschwind D, Roeder K, Devlin B, State MW. Multiple recurrent de novo CNVs,

including duplications of the 7q11.23 Williams syndrome region, are strongly associated with autism. Neuron. 2011; 70:863–885. [PubMed: 21658581]

Schnell E, Bensen AL, Washburn EK, Westbrook GL. Neuroligin-1 overexpression in newborn granule cells in vivo. PloS one. 2012; 7:e48045. [PubMed: 23110172]

Shen K, Scheiffele P. Genetics and cell biology of building specific synaptic connectivity. Annu Rev Neurosci. 2010; 33:473–507. [PubMed: 20367446]

Shipman SL, Nicoll RA. Dimerization of postsynaptic neuroligin drives synaptic assembly via transsynaptic clustering of neurexin. Proc Natl Acad Sci U S A. 2012a; 109:19432–19437. [PubMed: 23129658]

Shipman SL, Nicoll RA. A subtype-specific function for the extracellular domain of neuroligin 1 in hippocampal LTP. Neuron. 2012b; 76:309–316. [PubMed: 23083734]

Siddiqui TJ, Craig AM. Synaptic organizing complexes. Current opinion in neurobiology. 2011; 21:132–143. [PubMed: 20832286]

Siddiqui TJ, Pancaroglu R, Kang Y, Rooyakkers A, Craig AM. LRRTMs and neuroligins bind neurexins with a differential code to cooperate in glutamate synapse development. J Neurosci. 2010; 30:7495–7506. [PubMed: 20519524]

Song JY, Ichtchenko K, Sudhof TC, Brose N. Neuroligin 1 is a postsynaptic cell-adhesion molecule of excitatory synapses. Proc Natl Acad Sci U S A. 1999; 96:1100–1105. [PubMed: 9927700]

Soykan T, Schneeberger D, Tria G, Buechner C, Bader N, Svergun D, Tessmer I, Poulopoulos A, Papadopoulos T, Varoqueaux F, Schindelin H, Brose N. A conformational switch in collybistin determines the differentiation of inhibitory postsynapses. EMBO J. 2014

Sudhof TC. Neuroligins and neurexins link synaptic function to cognitive disease. Nature. 2008; 455:903–911. [PubMed: 18923512]

Sugita S, Saito F, Tang J, Satz J, Campbell K, Sudhof TC. A stoichiometric complex of neurexins and dystroglycan in brain. J Cell Biol. 2001; 154:435–445. [PubMed: 11470830]

Uemura T, Lee SJ, Yasumura M, Takeuchi T, Yoshida T, Ra M, Taguchi R, Sakimura K, Mishina M. Trans-synaptic interaction of GluRdelta2 and Neurexin through Cbln1 mediates synapse formation in the cerebellum. Cell. 2010; 141:1068–1079. [PubMed: 20537373]

Varoqueaux F, Aramuni G, Rawson RL, Mohrmann R, Missler M, Gottmann K, Zhang W, Sudhof TC, Brose N. Neuroligins determine synapse maturation and function. Neuron. 2006; 51:741–754. [PubMed: 16982420]

Varoqueaux F, Jamain S, Brose N. Neuroligin 2 is exclusively localized to inhibitory synapses. Eur J Cell Biol. 2004; 83:449–456. [PubMed: 15540461]

Woo J, Kwon SK, Choi S, Kim S, Lee JR, Dunah AW, Sheng M, Kim E. Trans-synaptic adhesion between NGL-3 and LAR regulates the formation of excitatory synapses. Nature neuroscience. 2009; 12:428–437.

Yu W, De Blas AL. Gephyrin expression and clustering affects the size of glutamatergic synaptic contacts. J Neurochem. 2008; 104:830–845. [PubMed: 18199120]

Yu W, Jiang M, Miralles CP, Li RW, Chen G, de Blas AL. Gephyrin clustering is required for the stability of GABAergic synapses. Mol Cell Neurosci. 2007; 36:484–500. [PubMed: 17916433]

Zoghbi HY. Postnatal neurodevelopmental disorders: meeting at the synapse? Science. 2003; 302:826–830. [PubMed: 14593168]

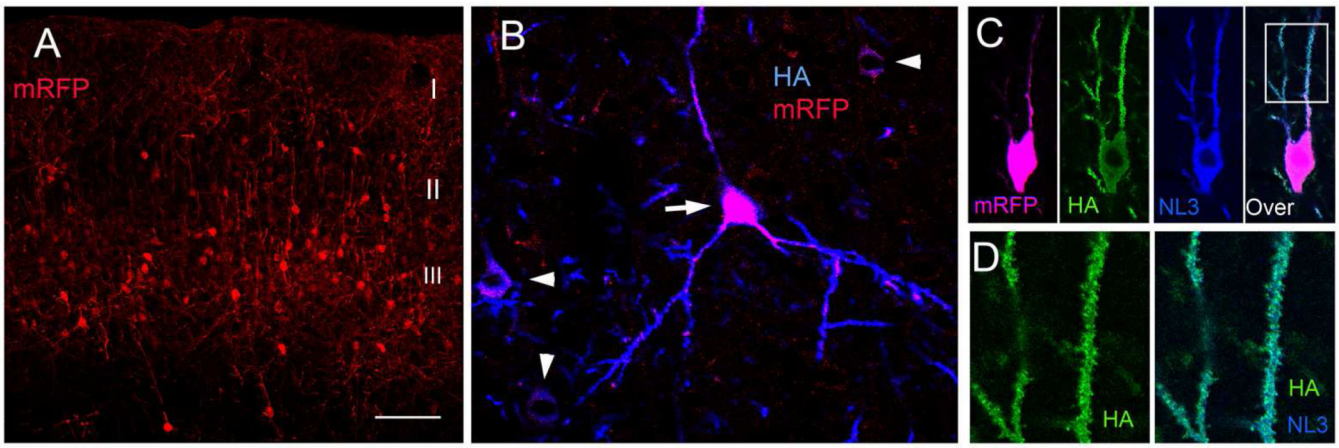

Figure 1. In the cerebral cortex, many neuronal precursors that have been transfected *in utero* with NL3, migrate to the appropriate cortical layers and differentiate into adult neurons overexpressing NL3

(A) Neurons that have been IUEP at E14 with both HA-NL3 and mRFP radially migrate to layers II–III of the rat cerebral cortex; **(B)** Double-label fluorescence. Transfected neurons overexpress both HA-NL3 (blue, HA fluorescence) and mRFP fluorescence (red). The arrow points to a neuron with high expression of mRFP and HA-NL3. Arrowheads point to neurons expressing lower levels of both mRFP and HA-NL3; **(C)** Triple-label immunofluorescence shows that individual neurons that have mRFP fluorescence (red), also show anti-HA fluorescence (green) and NL3 fluorescence (blue). Over is the overlay; (D) higher magnification of the boxed area. Note the presence of HA and NL3 immunofluorescence in both dendritic spines and dendritic shaft. The right side panel shows the overlay of HA and NL3 immunofluorescence. Ms anti-HA, Rb anti-NL3 and Rb anti-RFP were used. Scale bar is 100 μm in A, 33 μm in B and C and 10 μm in D.

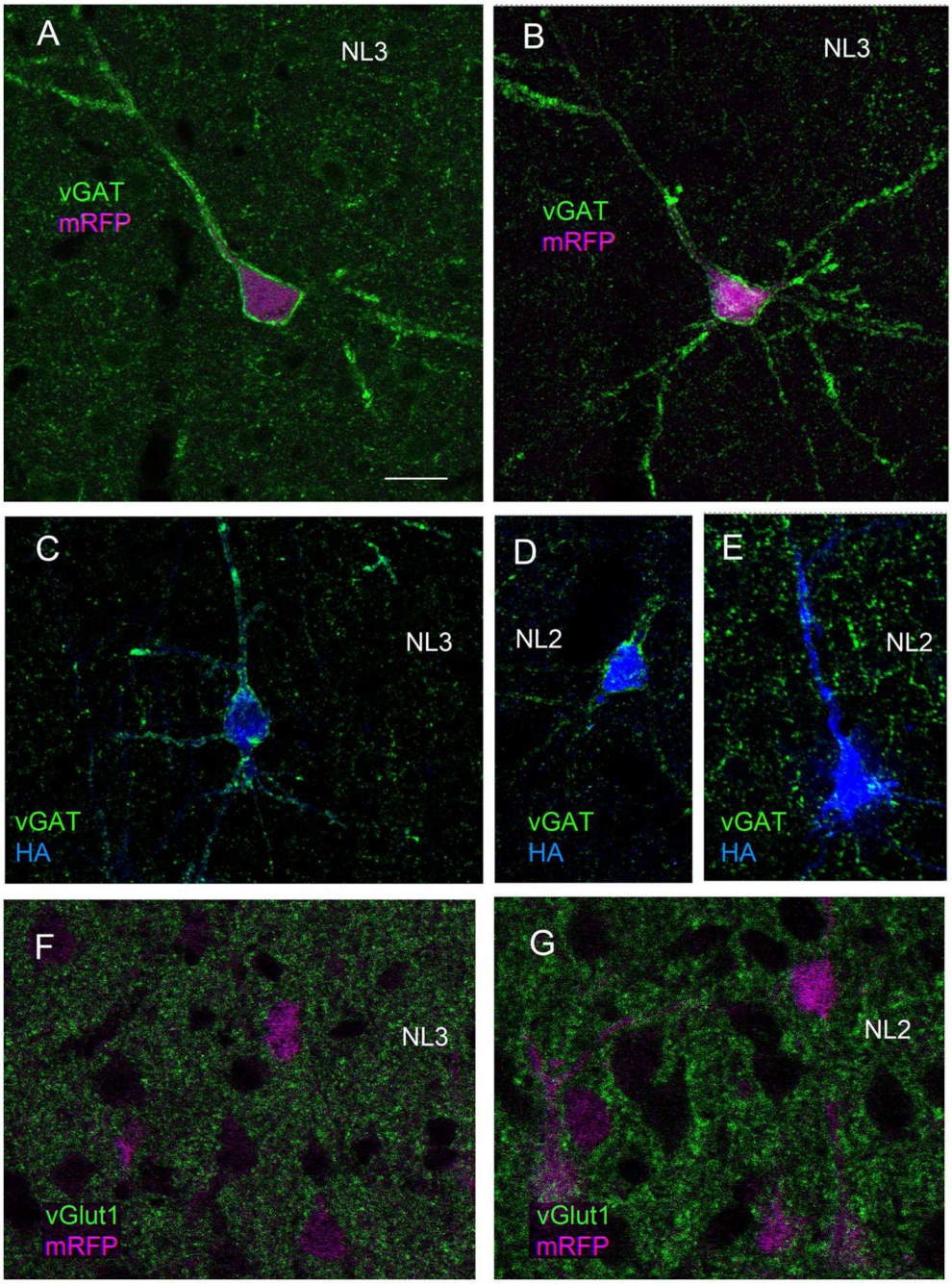

Figure 2. In the cerebral cortex, the levels of vGAT are highly increased in the GABAergic contacts that NL3-overexpressing neurons receive. In contrast, the levels of vGlut1 in the glutamatergic contacts are not affected

(A–C) vGAT fluorescence (green) of neurons overexpressing HA-NL3 (blue, HA fluorescence) and mRFP fluorescence (red). A: single optical section; B: average projection of a stack of 39 optical sections; C: average projection of a stack of 29 optical sections; **(D and E)** vGAT fluorescence (green) of neurons overexpressing HA-NL2 (blue, HA fluorescence). D: average projection of a stack of 26 optical sections; E: single optical section; **(F)** vGlut1 fluorescence (green) of neurons overexpressing HA-NL3 and mRFP

(red). **(G)** vGlut1 fluorescence (green) of neurons overexpressing HA-NL2 and mRFP (red). Single optical sections are 0.5μm thick. All the neurons overexpressing mRFP and HA-NL3 or HA-NL2 show both mRFP fluorescence (red) and HA immunofluorescence (blue). Rb anti-vGAT, Rb anti-vGlut1 and Ms anti-HA were used. Scale bar is 20 μm for all panels.

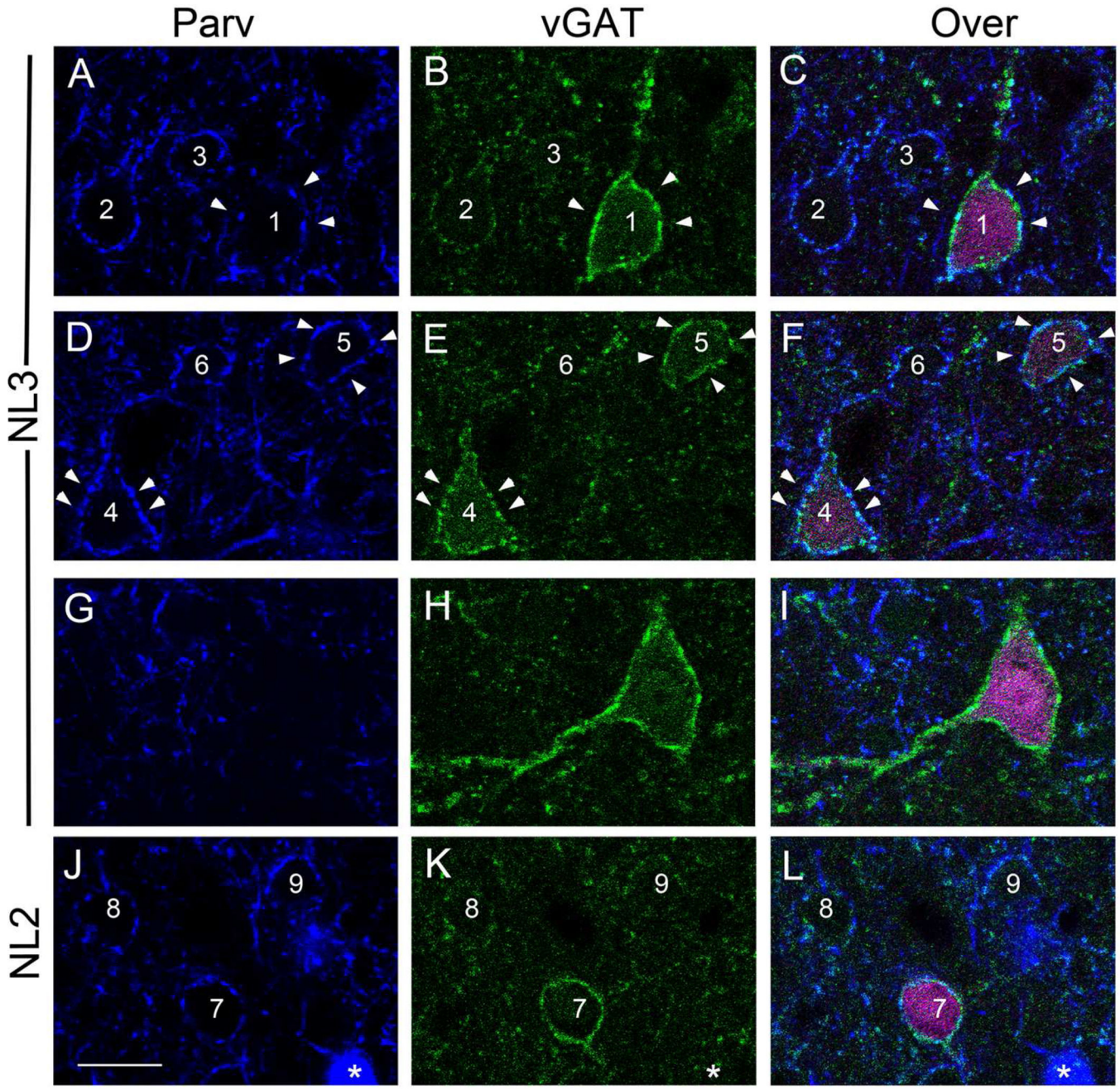

Figure 3. In the cerebral cortex, the innervation of neurons overexpressing NL3 by parvalbumin-containing GABAergic boutons is not significantly affected compared to non-transfected neurons

(A–C) Neuron 1 overexpressing HA-NL3 (red) shows an increase of vGAT fluorescence (green) from innervating GABAergic boutons but shows no increase in parvalbumin (blue) compared to non-transfected neurons 2 and 3. In neuron 1, some of the presynaptic boutons with vGAT fluorescence show co-localizing parvalbumin fluorescence (arrowheads). Note in A that non-transfected neurons 2 and 3, with normal (lower than transfected) levels of vGAT in the innervating GABAergic terminals show more parvalbumin around their somas than the transfected neuron 1; **(D–F)** NL3 transfected neurons 4 and 5 show heavy

innervation by parvalbumin and vGAT terminals, but in the case of parvalbumin, the difference with non-transfected neuron 6 is not apparent. Arrowheads show GABAergic boutons containing both vGAT and parvalbumin; **(G–I)** Example of a HA-NL3-transfected neuron with high vGAT fluorescence in the innervating boutons but with no parvalbumin fluorescence; **(J–L)** NL2-transfected neuron (neuron 7, red) has high levels of vGAT fluorescence in the innervating GABAergic terminals but the levels of parvalbumin fluorescence are not higher than in non-transfected neurons 8 and 9. The asterisk shows the soma of a parvalbumin interneuron. Ms anti-parvalbumin and GP anti-vGAT were used. Scale bar is 20 μm for all panels.

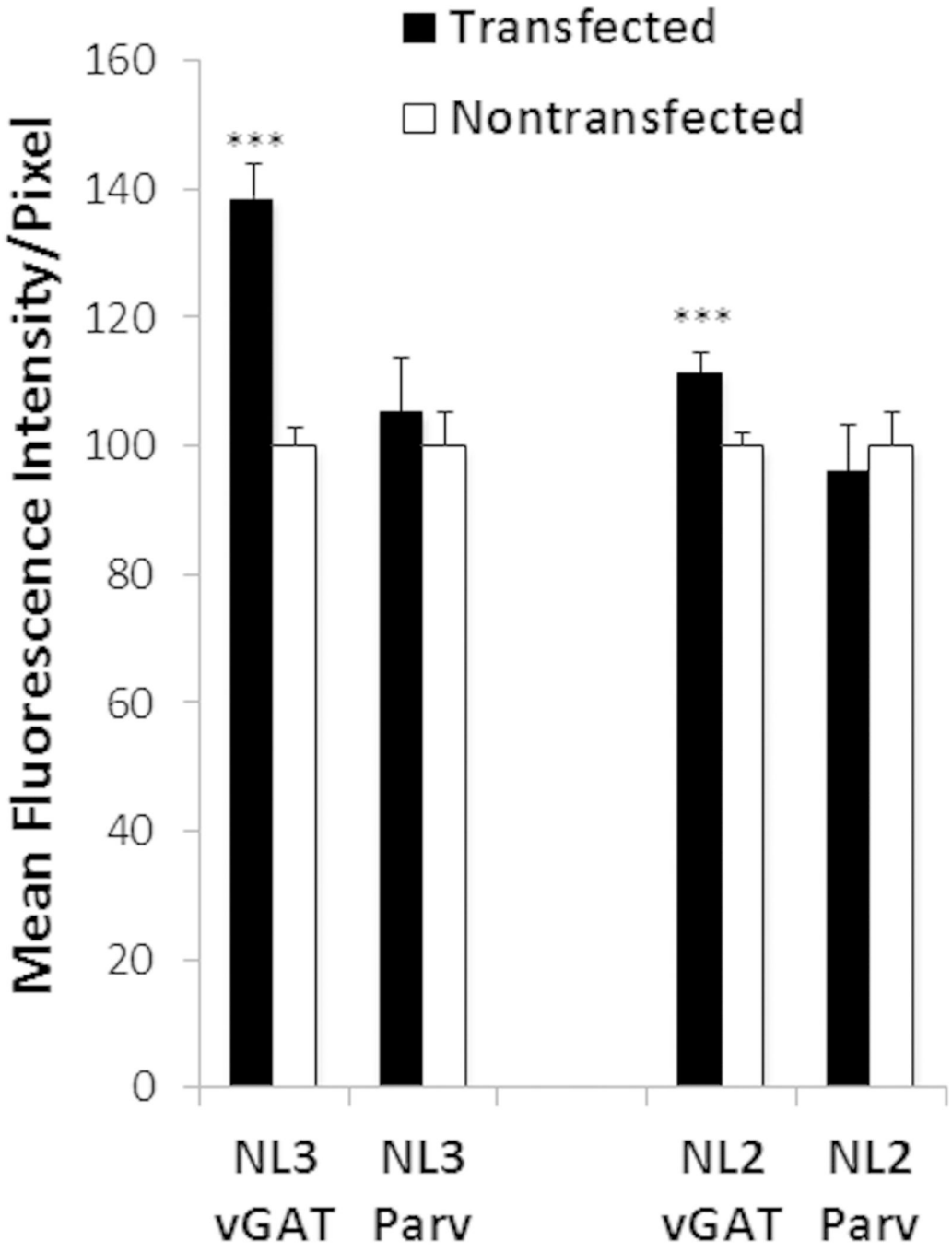

Figure 4. Quantification of vGAT and parvalbumin fluorescence in the surface of the soma of NL3 and NL2 overexpressing neurons

Mean Fluorescence Intensity per pixel of vGAT and parvalbumin in the surface of the soma of NL3- and NL2- transfected neurons normalized to that of the corresponding sister non-transfected neurons (100%). *** $p<0.001$. Values are normalized to that of non-transfected sister neurons from the same image (100%).

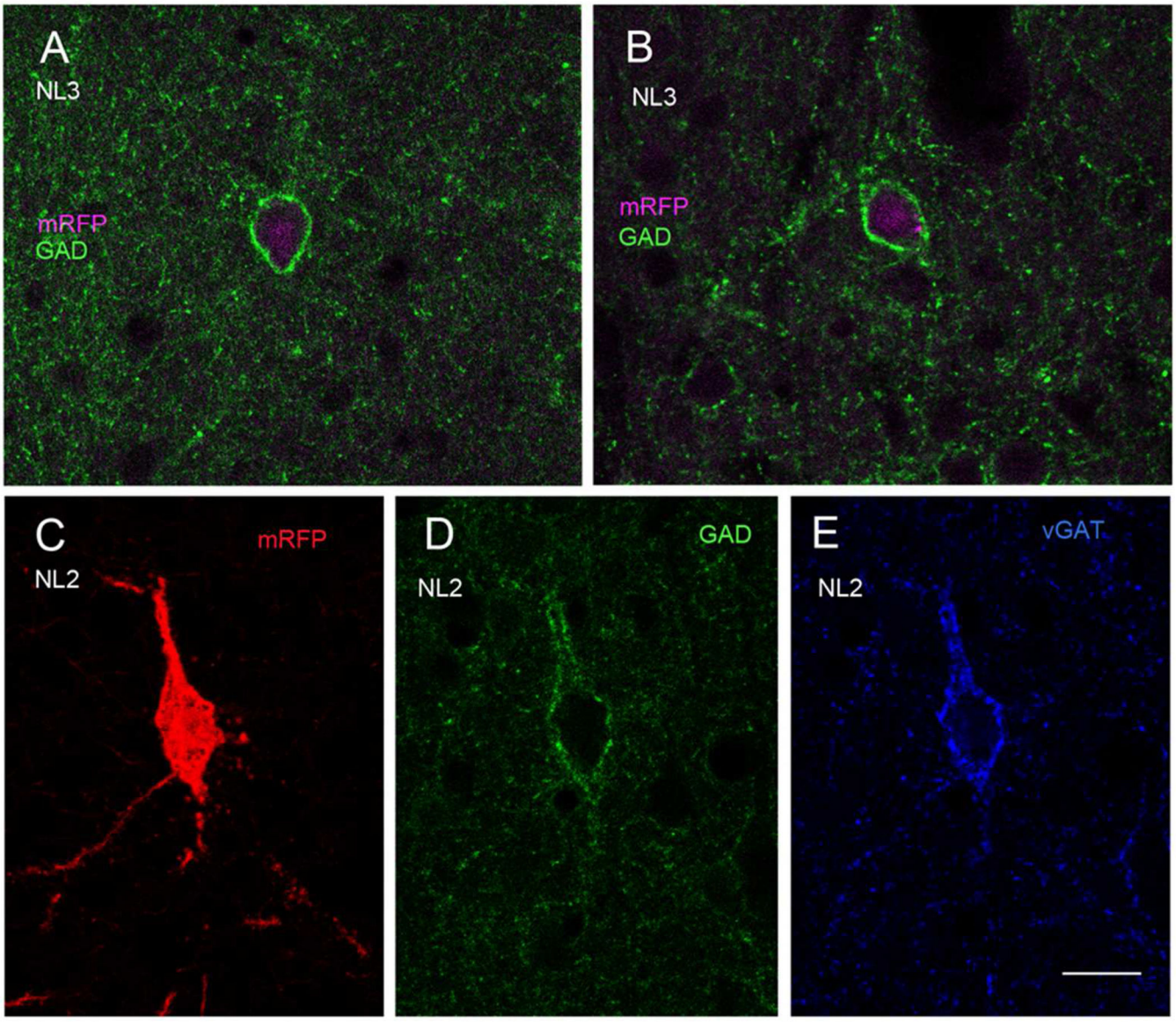

Figure 5. The NL3 overexpressing neurons show increased fluorescence of both vGAT and GAD in their GABAergic contacts

(A, B) Neurons in the cerebral, cortex that have been IUEP with HA-NL3 and mRFP (red) show increase GAD fluorescence (green) from innervating GABAergic terminals. **(C–E)** Neurons in the cerebral, cortex that have been IUEP with HA-NL2 and mRFP (red) show increased GAD (green) and vGAT (blue) fluorescence. Sheep anti-GAD and Ms anti-DsRed were used in A–B. Rb anti-RFP, Ms anti-GAD and GP anti-vGAT were used in Fig C–E. Scale bar is 20 μm for all panels

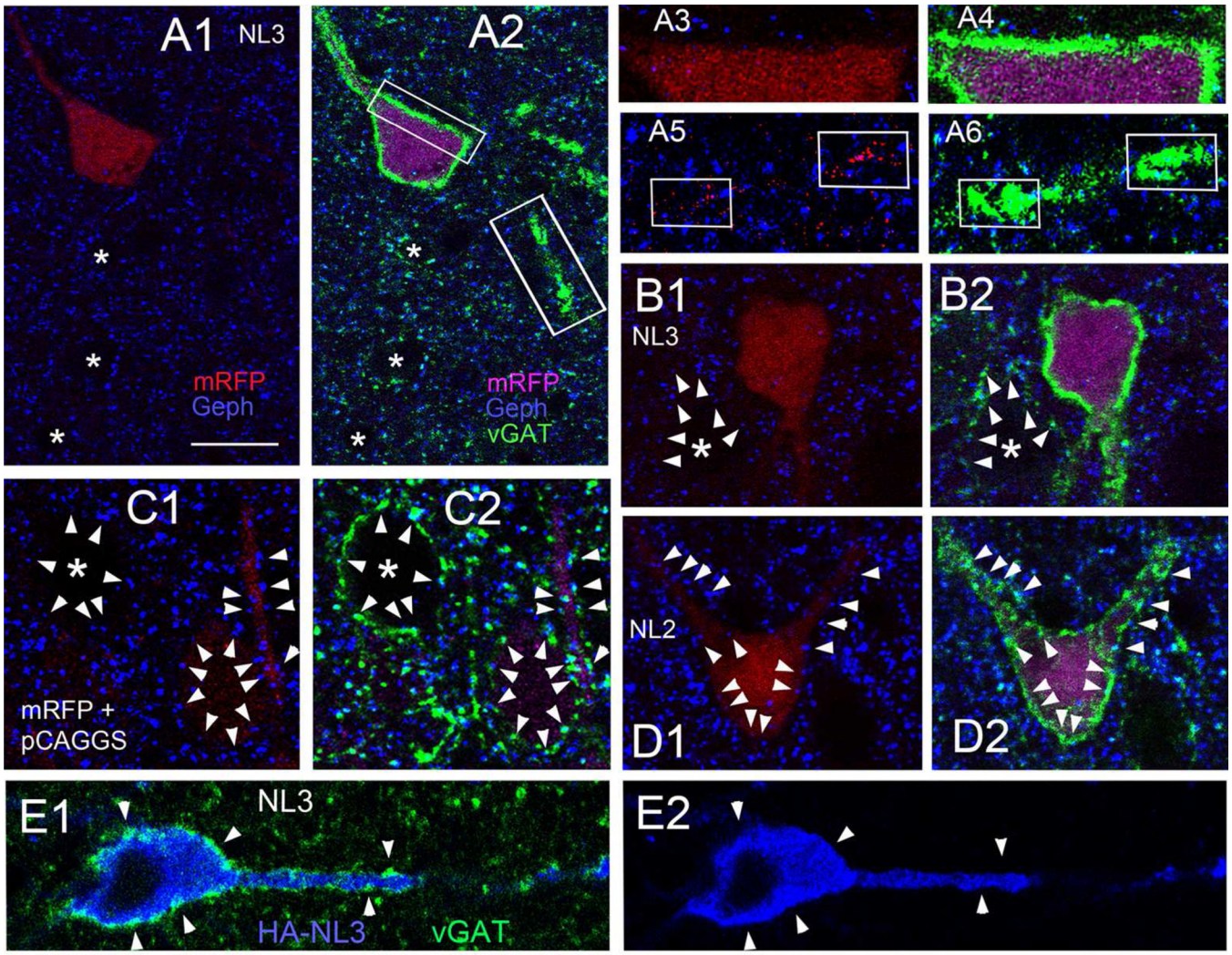

Figure 6. In the cerebral cortex, the neurons that overexpress NL3 frequently do not show gephyrin clusters juxtaposed to the vGAT-containing contacting boutons

(A, B) Triple-label immunofluorescence with anti-gephyrin (blue), anti-vGAT (green) and mRFP (red) in NL3-overexpressing neurons. In these neurons there are very few postsynaptic gephyrin clusters juxtaposed to the vGAT fluorescence. A1 and A2 show a NL3-transfected neuron (red). B1 and B2 show another NL3-transfected neuron (red). A3 and A4 show at higher magnification the soma, and A5 and A6 a dendrite, with high vGAT labeling in the GABAergic contacts, from the corresponding boxed areas in A2. Asterisks in A1, A2, B1 and B2 indicate some non-transfected neurons. Arrowheads in these and other panels in the figure indicate juxtaposition between vGAT (green) and gephyrin (blue); **(C)** A non-transfected neuron (asterisk) and a mRFP-transfected neuron (red) from an animal IUEP with both mRFP and an empty pCAGGS control plasmid (with no NL3) show considerable juxtaposition between vGAT (green) and gephyrin (blue) in soma and dendrites (arrowheads). **(D)** Neurons from an animal IUEP with NL2 show increased vGAT (green) and frequent juxtaposition of vGAT with gephyrin (blue). For the pair of images A–D, the left side panel shows the overlay of gephyrin and mRFP while the right-side panel shows the overlay of vGAT1, gephyrin and mRFP fluorescence. **(E)** A neuron overexpressing HA-

NL3. There is no evident accumulation of HA-NL3 (blue) juxtaposed (arrowheads) to vGAT-containing contacts in soma or dendrites. For the pair E1–E2 the left side panel shows the overlay of vGAT (green) and HA-NL3 (blue) while the right-side panel shows HA-NL3 (blue). Ms anti-gephyrin and Rb anti-vGAT were used in A–D. Ms anti-HA and Rb anti-vGAT were used in E. Scale bar is 20 μm for A1 and A2; 17 μm for E1 and E2; 12 μm for B1, B2, C1, C2, D1 and D2 and 8 μm for A3, A4, A5 and A6.

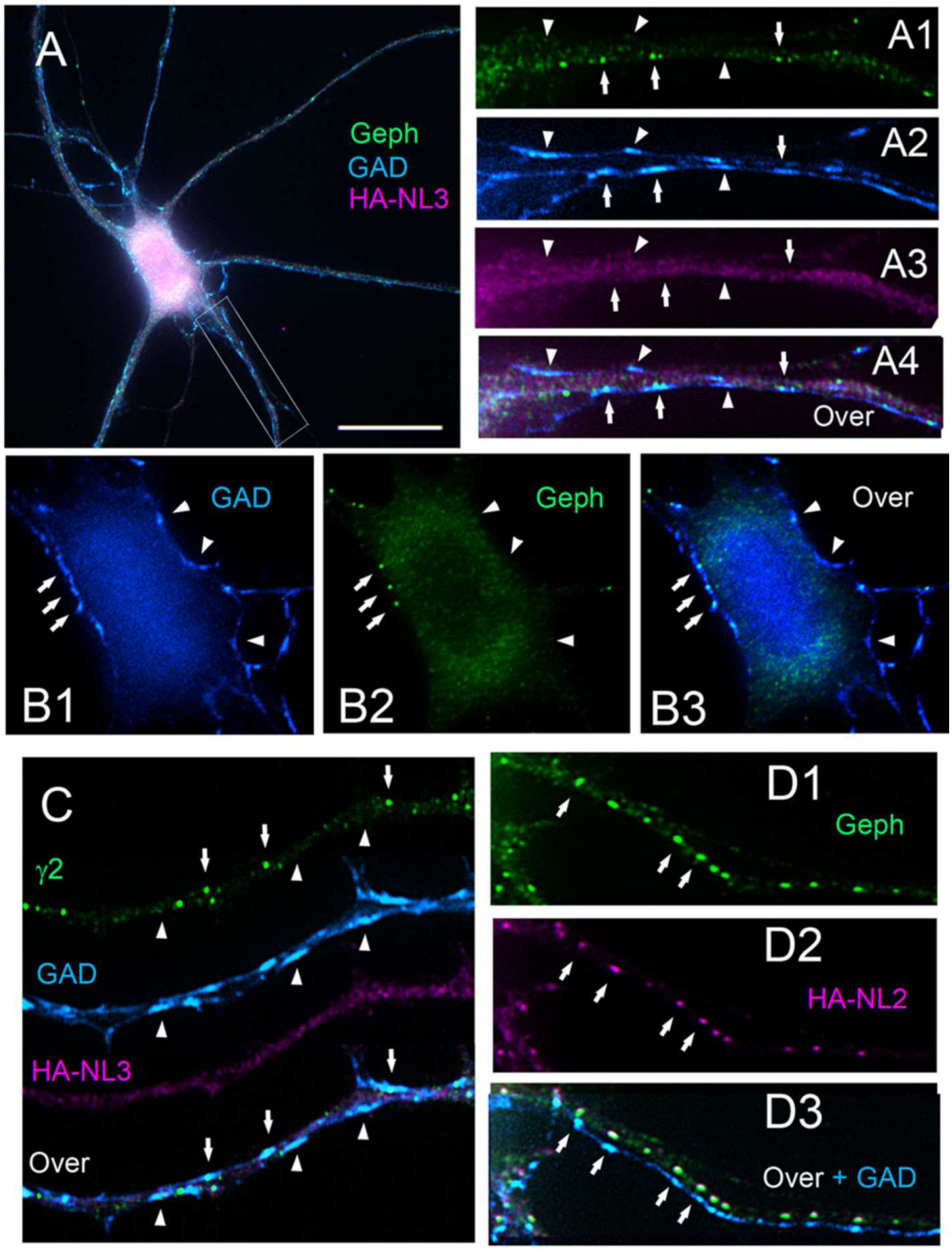

Figure 7. GAD-boutons contacting cultured neurons overexpressing HA-NL3 frequently do not have juxtaposed gephyrin or γ2-GABA$_A$R clusters. Moreover, HA-NL3 does not form clusters while HA-NL2 forms postsynaptic clusters at GABAergic synapses

(A, B) Neurons that overexpress HA-NL3 (A3, red) show prominent GAD fluorescence (A2, blue) in the GABAergic boutons contacting the transfected neurons. Nevertheless, many GAD positive puncta do not have juxtaposed gephyrin clusters (A1, green) in the dendrites (A1–A4) or the soma (B1–B3) of the transfected neurons (arrowheads). Arrows point to GAD positive contacts that have juxtaposed gephyrin. Transfected neurons are identified by anti-HA fluorescence (red). Neurons transfected with HA-NL3 do not form

HA-NL3 clusters (A3, red) at GABAergic synapses (arrows); Panels A1–A4 correspond to boxed area in panel A. **(C)** The GAD boutons (blue) that contact HA-NL3 overexpressing neurons frequently do not have associated γ2 $GABA_AR$ clusters (green, arrowheads). Some GAD contacts have juxtaposed γ2 $GABA_AR$ clusters (arrows). **(D)** Neurons overexpressing HA-NL2 show postsynaptic clustering of HA-NL2 (D2, red, anti-HA fluorescence) co-localizing with gephyrin clusters (D1, green), being juxtaposed to GAD-containing presynaptic boutons (D3, blue). D3 shows the overlay of the green and red fluorescence channels while the blue channel was slightly displaced downwards for better appreciation of the synaptic contacts. Ms anti-HA, Rb anti-gephyrin and Sh anti-GAD were used in A–B and D. Ms anti-HA, Rb anti-γ2 and Sh anti-GAD were used in C. Scale bar is 25 μm for A; 10 μm for B1–B3 and 8.3 μm for A1–A4, C and D1–D3.

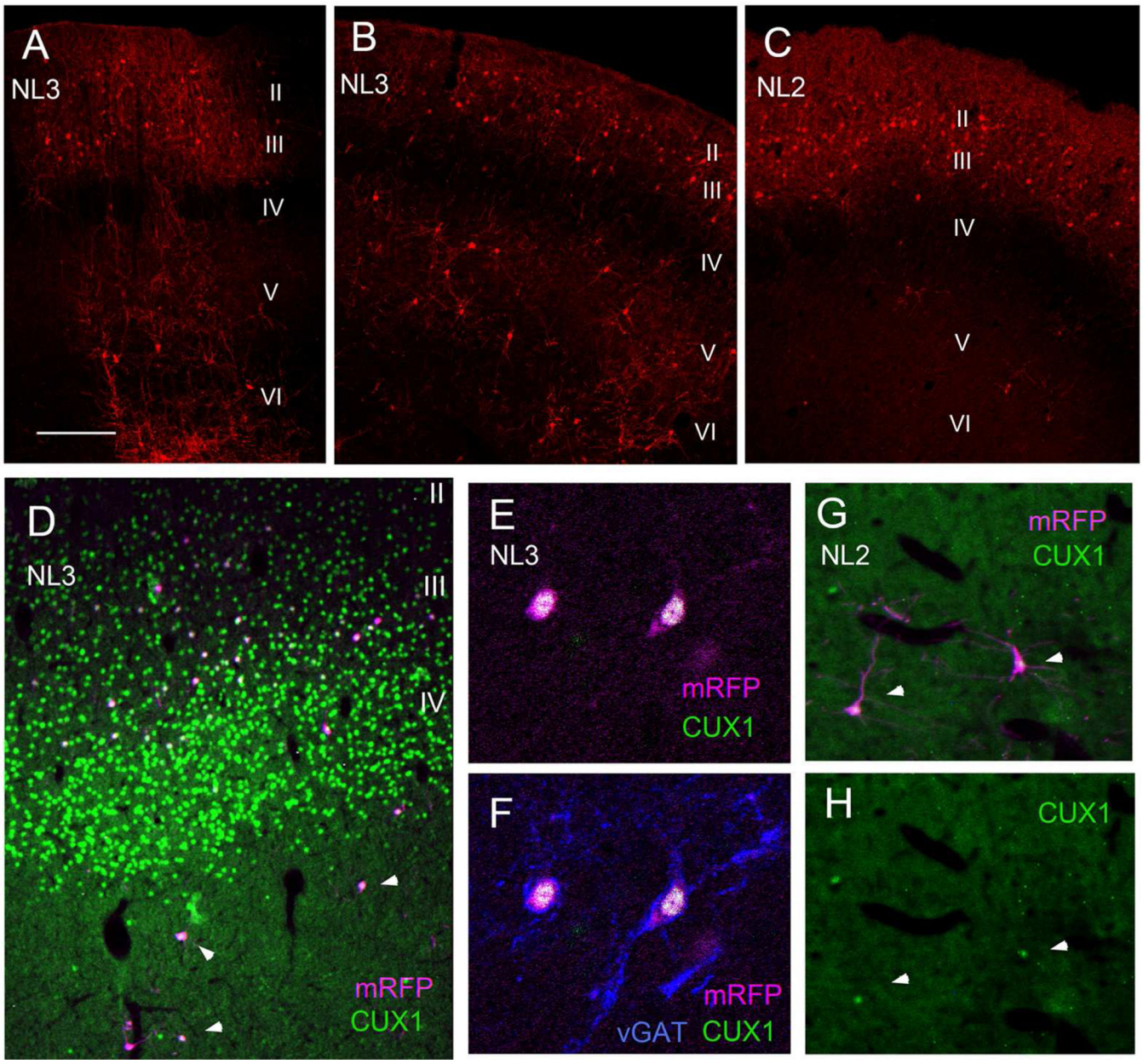

Figure 8. Some NL3 overexpressing neurons show impaired radial migration in the cerebral cortex

(A, B) Some neurons overexpressing NL3 and mRFP fail to migrate to upper layers II–III, remaining in the lower layers V and VI. **(C)** The large majority of neurons overexpressing NL2 and mRFP migrate to layers II–III and only a few remain in the lower layers. Note in A and C that the barrels of the somatosensory cortex are revealed because of the lack of labeling in layer IV. **(D)** Neurons overexpressing NL3 and mRFP (red) that migrate to layers II and III and the ones that fail to migrate to layers II–III remaining in lower layers show expression of CUX1 in the nucleus (green). Arrowheads point to transfected neurons in the lower layers with CUX1 expression. **(E, F)** Show two transfected neurons (red) that remain in the lower layers (arrowheads) and that also express CUX1 (green). These neurons show

increased vGAT fluorescence (blue) in the boutons contacting these neurons. **(G, H)** NL2 and mRFP co-overexpressing neurons (red) that are present in lower layers (layer V) of the cerebral cortex also express CUX1 (green). Rb anti-RFP was used in A–C. Ms anti-DsRed and Rb anti-CUX1 were used in D–H. In addition, GP anti-vGAT was used in F. Scale bar is 250 μm in A–C; 150 μm in D; 30 μm in E and F and 100 μm in G and H.

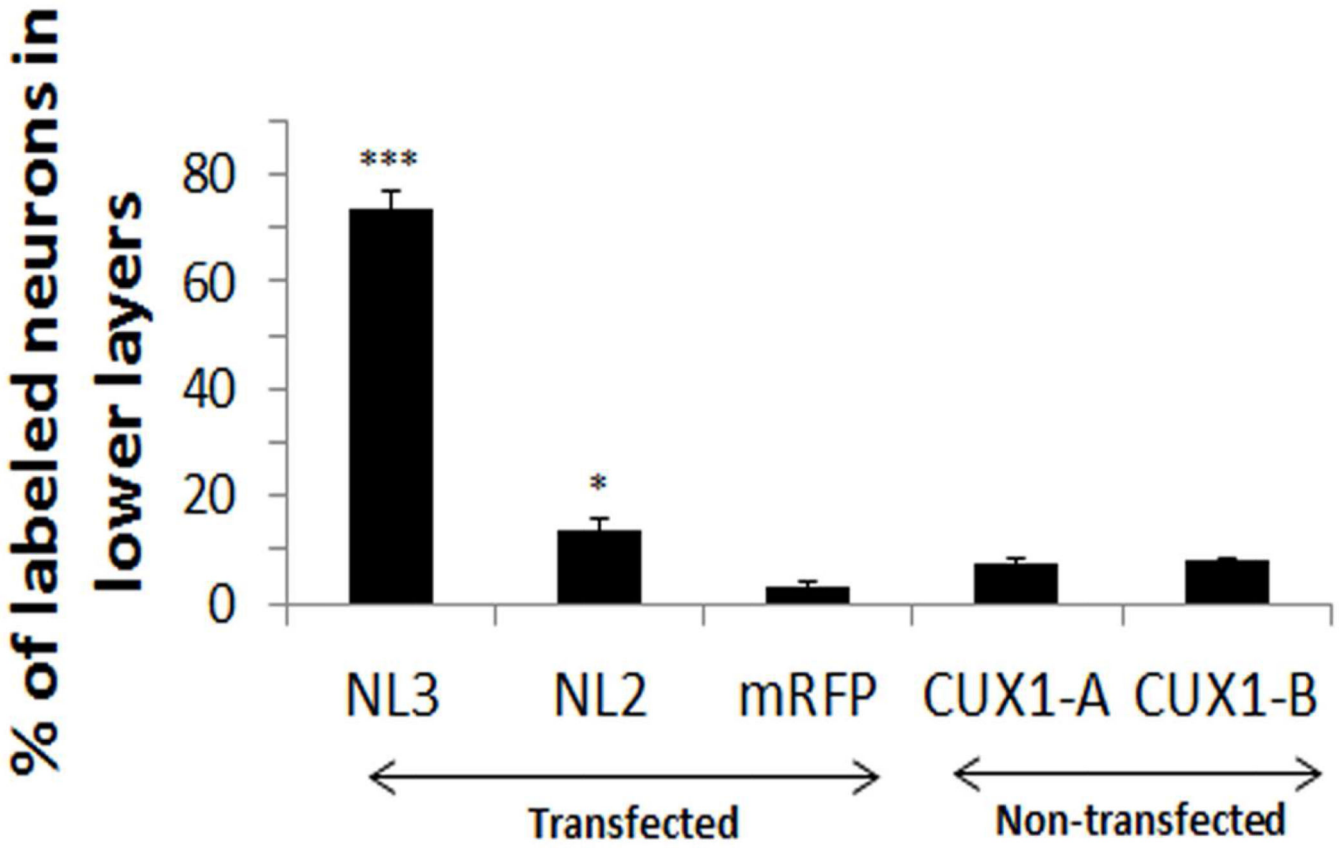

Figure 9. Quantification of labeled neurons that remain in the lower layers of the cerebral cortex

Values are given as percentage of labeled neurons in the lower layers (layers V, VI and white matter). The 100% values are the total number of labeled neurons in layers I–VI and white matter. NL3, NL2 or mRFP correspond to neurons transfected with NL3 (and mRFP), NL2 (and mRFP) or mRFP respectively. CUX1-A corresponds to non-transfected neurons that express CUX1 in the IUEP brains. CUX1-B corresponds to neurons that express CUX1 in brains of animals not subjected to IUEP. *** $p<0.001$; *$p<0.05$ in ANOVA Tukey-Kramer Multiple comparisons test.

TABLE 1

Primary Antibodies Used

Antigen	Immunogen	Manufacturer, Catalog #, RRID, Species, mono/polyclonal	Concentration
CUX1	amino acids 1111–1332 of CDP of mouse origin.	Santa Cruz Biotechnology; sc-13024; AB_2261231; Rabbit; Polyclonal	1:500
γ2 subunit of the $GABA_A$ Receptor	synthetic peptide QKSDDDYEDYASNKT	AB_2314477; Rabbit; Polyclonal	1:10[1];1:75[2]
GAD65	purified rat GAD	Dr. Irwin J. Kopin; lot#1440-4; AB_2314493; Sheep; Polyclonal	1:500[1];1:600[2]
GAD65	purified rat GAD	Developmental Studies Hybridoma Bank University of Iowa; GAD-6; AB_2314499; Mouse; Monoclonal	1:25
Gephyrin	N-terminus of gephyrin, surrounding phospho-serines 268 and 270.	Synaptic Systems; 147021; AB_1279448; Mouse; Monoclonal	1:200
Gephyrin	recombinant protein containing the C-terminal end of rat gephyrin (aa 518 – 736).	Synaptic Systems; 147003; AB_887718; Rabbit; Polyclonal	1:1,000
HA	synthetic peptide CYPYDVPDYASL	Covance; MMS-101R; AB_10063630; Mouse; Monoclonal	1:500
NL3	synthetic peptide CEAGPPHDTLRLTALPDYT corresponding to aa 775–793	Covance custom made; Rabbit; No RRID; Polyclonal	1:500
Parvalbumin	frog muscle parvalbumin	Sigma Aldrich; P3088; AB_477329; Mouse; Monoclonal	1:2,000
vGAT	Strep-Tag® fusion protein of rat vGAT (aa 2 – 115)	Synaptic Systems; 131004; AB_887873; Guinea Pig; Polyclonal	1:1,000
vGAT	synthetic peptide AEPPVEGDIHYQR (aa 75 – 87 in rat)	Synaptic Systems; 131003; AB_887869; Rabbit; Polyclonal	1:1,000
vGLUT1	Synthetic peptide corresponding to amino acids 542–560 of rat vGLUT1	EMD Millipore; AB5905; AB_2301751; Guinea Pig; Polyclonal	1:10,000

[1] IF with brain slices

[2] IF with neuronal cultures